

1
2 **Mitochondrial respiratory states and rates:**
3 **Building blocks of mitochondrial physiology Part 1**
4

5 **COST Action CA15203 MitoEAGLE preprint** Version: 2018-09-24(42)

6 Corresponding author: Gnaiger E

7 Co-authors:

8 Aasander Frostner E, Abumrad NA, Acuna-Castroviejo D, Adams SH, Ahn B, Ali SS, Alves MG,
9 Amati F, Amoedo ND, Aral C, Arandarčikaitė O, Arnould T, Avram VF, Bailey DM, Bajpeyi S,
10 Bakker BM, Bastos Sant'Anna Silva AC, Battino M, Bazil J, Beard DA, Bednarczyk P, Ben-Shachar
11 D, Bergdahl A, Bernardi P, Bishop D, Blier PU, Boetker HE, Boros M, Borsheim E, Borutaitė V,
12 Bouillaud F, Bouitbir J, Breton S, Brown DA, Brown GC, Brown RA, Brozinick JT, Buettner GR,
13 Burtscher J, Calabria E, Calbet JA, Calzia E, Cannon DT, Canto AC, Cardoso LHD, Carvalho E,
14 Casado Pinna M, Cassina AM, Castro L, Cavalcanti-de-Albuquerque JP, Cervinkova Z, Chabi B,
15 Chakrabarti L, Chaurasia B, Chen Q, Chicco AJ, Chinopoulos C, Chowdhury SK, Cizmarova B,
16 Clementi E, Coen PM, Coker RH, Collin A, Crisóstomo L, Dambrova M, Danhelovska T, Darveau
17 CA, Das AM, Dash RK, Davis MS, De Goede P, De Palma C, Dembinska-Kiec A, Di Marcello M,
18 Dias TR, Distefano G, Doerrier C, Drahota Z, Dubouchaud H, Duchen MR, Dumas JF, Durham WJ,
19 Dymkowska D, Dyrstad SE, Dyson A, Dzialowski EM, Ehinger J, Elmer E, Endlicher R, Engin AB,
20 Escames G, Fell DA, Ferko M, Ferreira JCB, Ferreira R, Fessel JP, Filipovska A, Fisar Z, Fischer M,
21 Fisher G, Fisher JJ, Fornaro M, Galina A, Galkin A, Galli GL, Gan Z, Garcia-Roves PM, Garcia-
22 Souza LF, Garipi E, Garlid KD, Garrabou G, Garten A, Gastaldelli A, Genova ML, Giovarelli M,
23 Gonzalez-Armenta JL, Gonzalo H, Goodpaster BH, Gorr TA, Gourlay CW, Granata C, Grefte S,
24 Gueguen N, Gumeni S, Haas CB, Haavik J, Haendeler J, Hamann A, Han J, Han WH, Hancock CR,
25 Hand SC, Hargreaves IP, Harrison DK, Heales SJR, Hellgren KT, Hepple RT, Hernansanz-Agustin P,
26 Hickey AJ, Hoel F, Holland OJ, Holloway GP, Hoppel CL, Hoppel F, Houstek J, Huete-Ortega M,
27 Iglesias-Gonzalez J, Irving BA, Iyer S, Jackson CB, Jadiya P, Jang DH, Jang YC, Jansen-Dürr P,
28 Jarmuszkiewicz W, Jaspersen NR, Jha RK, Jurk D, Kaambre T, Kaczor JJ, Kainulainen H, Kandel
29 SM, Kane DA, Kappler L, Karabatsiakakis A, Karkucinska-Wieckowska A, Keijer J, Keller MA,
30 Keppner G, Khamoui AV, Klepinin A, Klingenspor M, Komlodi T, Koopman WJH, Kopitar-Jerala N,
31 Kowaltowski AJ, Kozlov AV, Krajcova A, Krako Jakovljevic N, Kristal BS, Kuang J, Kucera O,
32 Kuka J, Kwak HB, Kwast K, Laasmaa M, Labieniec-Watala M, Lai N, Land JM, Lane N, Laner V,
33 Lanza IR, Larsen TS, Lavery GG, Lee HK, Leeuwenburgh C, Lemieux H, Lenaz G, Lerfall J, Li PA,
34 Liepins E, Liu J, Lucchinetti E, Macedo MP, MacMillan-Crow LA, Makarova E, Makrečka-Kuka M,
35 Malik A, Markova M, Martin DS, Mazat JP, McKenna HT, Menze MA, Merz T, Meszaros AT,
36 Methner A, Michalak S, Moellering DR, Moiso N, Molina AJA, Montaigne D, Moore AL, Moreau K,
37 Moreno-Sánchez R, Moreira BP, Mracek T, Muntane J, Muntean DM, Murray AJ, Nair KS, Nehlin
38 JO, Nemeč M, Neuffer PD, Neuzil J, Newsom S, Nozickova K, O'Brien KA, O'Gorman D, Olgar Y,
39 Oliveira MF, Oliveira MT, Oliveira PF, Oliveira PJ, Orynbayeva Z, Osiewacz HD, Ounpuu L, Pak
40 YK, Pallotta ML, Palmeira CM, Parajuli N, Passos JF, Passrugger M, Patel HH, Pavlova N, Pecina P,
41 Pelnena D, Pereira da Silva Grilo da Silva F, Perez Valencia JA, Pesta D, Petit PX, Pettersen IKN,
42 Pichaud N, Piel S, Pietka TA, Pino MF, Pirkmajer S, Porter C, Porter RK, Pranger F, Prochownik EV,
43 Pulinilkunnit T, Puskarich MA, Puurand M, Quijano C, Radenkovic F, Radi R, Ramzan R, Rattan S,
44 Reboredo P, Rich PR, Renner-Sattler K, Rial E, Robinson MM, Roden M, Rodríguez-Enriquez S,
45 Rohlena J, Rolo AP, Ropelle ER, Røslund GV, Rossignol R, Rossiter HB, Rubelj I, Rybacka-
46 Mossakowska J, Saada A, Safaei Z, Salin K, Salvadego D, Sandi C, Sanz A, Sazanov LA, Scatena R,
47 Schartner M, Scheibye-Knudsen M, Schilling JM, Schlattner U, Schönfeld P, Schwarzer C, Scott GR,
48 Shabalina IG, Sharma P, Sharma V, Shevchuk I, Siewiera K, Silber AM, Silva AM, Sims CA, Singer
49 D, Skolik R, Smenes BT, Smith J, Soares FAA, Sobotka O, Sokolova I, Sonkar VK, Sowton AP,

Sparagna GC, Sparks LM, Spinazzi M, Stankova P, Stary C, Stelfa G, Stiban J, Stier A, Stocker R, Sumbalova Z, Suravajhala P, Swerdlow RH, Swiniuch D, Szabo I, Szewczyk A, Szibor M, Tanaka M, Tandler B, Tarnopolsky MA, Tavernarakis N, Tepp K, Thyfault JP, Tomar D, Towheed A, Tretter L, Trifunovic A, Trivigno C, Tronstad KJ, Trougakos IP, Tuncay E, Turan B, Tyrrell DJ, Urban T, Valentine JM, Vendelin M, Vercesi AE, Victor VM, Vieyra A, Vilks K, Villena JA, Vinogradov AD, Viscomi C, Vitorino RMP, Vogt S, Volani C, Volska K, Votion DM, Vujacic-Mirski K, Wagner BA, Ward ML, Warnsmann V, Wasserman DH, Watala C, Wei YH, Wieckowski MR, Williams C, Wohlgemuth SE, Wohlwend M, Wolff J, Wüst RCI, Yokota T, Zablocki K, Zaugg K, Zaugg M, Zdrzilova L, Zhang Y, Zhang YZ, Zíková A, Zischka H, Zorzano A, Zvejniece L

Updates and discussion:

http://www.mitoeagle.org/index.php/MitoEAGLE_preprint_2018-02-08

Correspondence: Gnaiger E

Chair COST Action CA15203 MitoEAGLE – <http://www.mitoeagle.org>

Department of Visceral, Transplant and Thoracic Surgery, D. Swarovski Research Laboratory,

Medical University of Innsbruck, Innrain 66/4, A-6020 Innsbruck, Austria

Email: mitoeagle@i-med.ac.at; Tel: +43 512 566796, Fax: +43 512 566796 20

Table of contents

Abstract - Executive summary

1. **Introduction** – Box 1: In brief: Mitochondria and Bioblasts

2. **Coupling states and rates in mitochondrial preparations**

2.1. *Cellular and mitochondrial respiration*

2.1.1. Aerobic and anaerobic catabolism and ATP turnover

2.1.2. Specification of biochemical dose

2.2. *Mitochondrial preparations*

2.3. *Electron transfer pathways*

2.4. *Respiratory coupling control*

2.4.1. Coupling

2.4.2. Phosphorylation, P_o, and P_o/O₂ ratio

2.4.3. Uncoupling

2.5. *Coupling states and respiratory rates*

2.5.1. **LEAK**

2.5.2. **OXPHOS**

2.5.3. **ET**

2.5.4. **ROX**

2.5.5. Quantitative relations

2.5.6. The steady-state

2.6. *Classical terminology for isolated mitochondria: States 1–5*

2.7. *Control and regulation*

3. **What is a rate?** – Box 2: Metabolic flows and fluxes: vectorial, vectorial, and scalar

4. **Normalization of rate per sample**

4.1. *Flow: per object*

4.1.1. Number concentration

4.1.2. Flow per object

4.2. *Size-specific flux: per sample size*

4.2.1. Sample concentration

4.2.2. Size-specific flux

4.3. *Marker-specific flux: per mitochondrial content*

4.3.1. Mitochondrial concentration and mitochondrial markers

4.3.2. mt-Marker-specific flux

5. **Normalization of rate per system**

5.1. *Flow: per chamber*

5.2. *Flux: per chamber volume*

5.2.1. System-specific flux

5.2.2. Advancement per volume

6. **Conversion of units**

7. **Conclusions** – Box 3: Recommendations for studies with mitochondrial preparations

References

111 **Abstract** As the knowledge base and importance of mitochondrial physiology to human health expands,
 112 the necessity for harmonizing the terminology concerning mitochondrial respiratory states and rates has
 113 become increasingly apparent. The chemiosmotic theory establishes the mechanism of energy
 114 transformation and coupling in oxidative phosphorylation. The unifying concept of the protonmotive
 115 force provides the framework for developing a consistent theoretical foundation of mitochondrial
 116 physiology and bioenergetics. We follow IUPAC guidelines on terminology in physical chemistry,
 117 extended by considerations on open systems and thermodynamics of irreversible processes. The
 118 concept-driven constructive terminology incorporates the meaning of each quantity and aligns concepts
 119 and symbols to the nomenclature of classical bioenergetics. We endeavour to provide a balanced view
 120 on mitochondrial respiratory control and a critical discussion on reporting data of mitochondrial
 121 respiration in terms of metabolic flows and fluxes. Uniform standards for evaluation of respiratory states
 122 and rates will ultimately support the development of databases of mitochondrial respiratory function in
 123 species, tissues, and cells. Clarity of concept and consistency of nomenclature facilitate effective
 124 transdisciplinary communication, education, and ultimately further discovery.

125
 126 *Keywords:* Mitochondrial respiratory control, coupling control, mitochondrial preparations,
 127 protonmotive force, uncoupling, oxidative phosphorylation, OXPHOS, efficiency, electron transfer, ET;
 128 electron transfer system, ETS; proton leak, LEAK, residual oxygen consumption, ROX, State 2, State
 129 3, State 4, normalization, flow, flux, O₂

131 **Executive summary**

132
 133 In view of the broad implications for health care, mitochondrial researchers face an increasing
 134 responsibility to disseminate their fundamental knowledge and novel discoveries to a wide range of
 135 stakeholders and scientists beyond the group of specialists. This requires implementation of a commonly
 136 accepted terminology within the discipline and standardization in the translational context. Authors,
 137 reviewers, journal editors, and lecturers are challenged to collaborate with the aim to harmonize the
 138 nomenclature in the growing field of mitochondrial physiology and bioenergetics, from evolutionary
 139 biology and comparative physiology to mitochondrial medicine. In the present communication we focus
 140 on the following concepts in mitochondrial physiology:

- 141 1. Aerobic respiration depends on the coupling of phosphorylation (ADP → ATP) to O₂ flux in
 142 catabolic reactions. Coupling in oxidative phosphorylation is mediated by the translocation of
 143 protons across the inner mitochondrial membrane through proton pumps generating or
 144 utilizing the protonmotive force, that is generated between the mitochondrial matrix and
 145 intermembrane compartment or outer mitochondrial space. Compartmental coupling
 146 distinguishes this vectorial component of oxidative phosphorylation from glycolytic
 147 fermentation as the counterpart of cellular core energy metabolism (**Figure 1**). Cell respiration
 148 is distinguished from fermentation: (1) Electron acceptors are supplied by external respiration
 149 for the maintenance of redox balance, whereas fermentation is characterized by an internal
 150 electron acceptor produced in intermediary metabolism. In aerobic cell respiration, redox
 151 balance is maintained by O₂ as the electron acceptor. (2) Compartmental coupling in vectorial
 152 oxidative phosphorylation contrasts to exclusively scalar substrate-level phosphorylation in
 153 fermentation.
- 154 2. When measuring mitochondrial metabolism, the contribution of fermentation and other cytosolic
 155 interactions must be excluded from analysis by disrupting the barrier function of the plasma
 156 membrane. Selective removal or permeabilization of the plasma membrane yields
 157 mitochondrial preparations—including isolated mitochondria, tissue and cellular
 158 preparations—with structural and functional integrity. Subsequently, extra-mitochondrial
 159 concentrations of fuel substrates, ADP, ATP, inorganic phosphate, and cations including H⁺
 160 can be controlled to determine mitochondrial function under a set of conditions defined as
 161 *coupling control states*. We strive to incorporate an easily recognized and understood, concept-
 162 driven terminology of bioenergetics with explicit terms and symbols that define the nature of
 163 respiratory states.
- 164 3. Mitochondrial coupling states are defined according to the control of respiratory oxygen flux by
 165 the protonmotive force. Capacities of oxidative phosphorylation and electron transfer are
 166 measured at kinetically saturating concentrations of fuel substrates, ADP and inorganic

phosphate, and O_2 , or at optimal uncoupler concentrations, respectively, in the absence of Complex IV inhibitors such as NO, CO, or H_2S . Respiratory capacity is a measure of the upper bound of the rate of respiration; it depends on the substrate type undergoing oxidation, and provides reference values for the diagnosis of health and disease, and for evaluation of the effects of Evolutionary background, Age, Gender and sex, Lifestyle and Environment.

Figure 1. Internal and external respiration

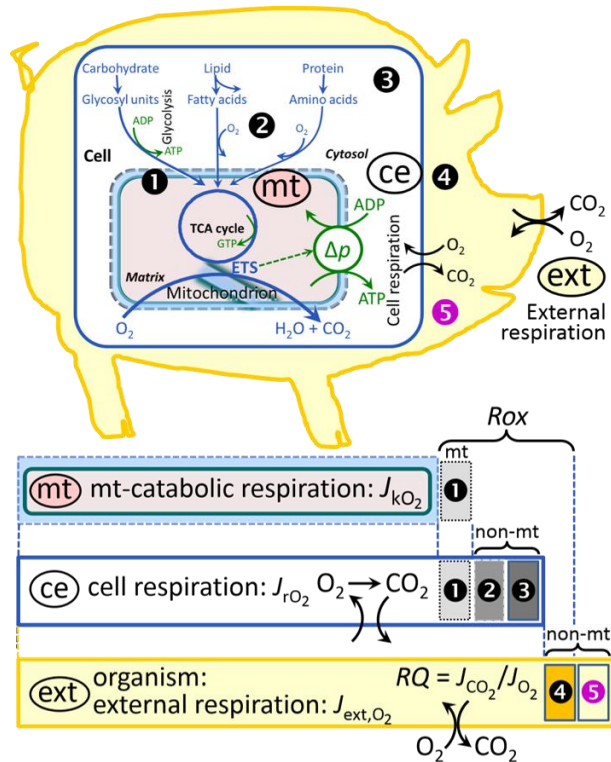
Mitochondrial respiration is the oxidation of fuel substrates (electron donors) and reduction of O_2 catalysed by the electron transfer system, ETS: (mt) mitochondrial catabolic respiration; (ce) total cellular O_2 consumption; and (ext) external respiration. All chemical reactions, r , that consume O_2 in the cells of an organism, contribute to cell respiration, J_{rO_2} . In addition to mitochondrial catabolic respiration, O_2 is consumed by:

1 Mitochondrial residual O_2 consumption, Rox .
 2 Non-mitochondrial O_2 consumption by catabolic reactions, particularly peroxisomal oxidases and microsomal cytochrome P450 systems. 3 Non-mitochondrial Rox by reactions unrelated to catabolism. 4 Extracellular Rox mt- Rox and non-mt Rox are measured without fuel substrate supply or after inhibiting the ETS. 5 Aerobic microbial respiration. Bars are not at a quantitative scale.

(mt) **Mitochondrial catabolic respiration**, J_{kO_2} , is the O_2 consumption by the mitochondrial ETS excluding Rox .

(ce) **Cell respiration**, J_{rO_2} , takes into account internal O_2 -consuming reactions, r , including catabolic respiration and Rox . Catabolic cell respiration is the O_2 consumption associated with catabolic pathways in the cell, including mitochondrial catabolism in addition to peroxisomal and microsomal oxidation reactions (2).

(ext) **External respiration** balances internal respiration at steady-state, including extracellular Rox (4) and aerobic respiration by the microbiome (5). O_2 is transported from the environment across the respiratory cascade, *i.e.*, circulation between tissues and diffusion across cell membranes, to the intracellular compartment. The respiratory quotient, RQ , is the molar CO_2/O_2 exchange ratio; when combined with the respiratory nitrogen quotient, N/O_2 (mol N given off per mol O_2 consumed), the RQ reflects the proportion of carbohydrate, lipid and protein utilized in cell respiration during aerobically balanced steady-states. Bicarbonate and CO_2 are transported in reverse to the extracellular milieu and the organismic environment. Hemoglobin provides the molecular paradigm for the combination of O_2 and CO_2 exchange, as do lungs and gills on the morphological level.



- Incomplete tightness of coupling, *i.e.*, some degree of uncoupling relative to the substrate-dependent coupling stoichiometry, is a characteristic of energy-transformations across membranes. Uncoupling is caused by a variety of physiological, pathological, toxicological, pharmacological and environmental conditions that exert an influence not only on the proton leak and cation cycling, but also on proton slip within the proton pumps and the structural integrity of the mitochondria. A more loosely coupled state is induced by stimulation of mitochondrial superoxide formation and the bypass of proton pumps. In addition, the use of protonophores represents an experimental uncoupling intervention to assess the transition from a well-coupled to a noncoupled state of mitochondrial respiration.
- Respiratory oxygen consumption rates have to be carefully normalized to enable meta-analytic studies beyond the question of a particular experiment. Therefore, all raw data should be published in a supplemental table or open access data repository. Normalization of rates for:

- 223 (1) the number of objects (cells, organisms); (2) the volume or mass of the experimental
 224 sample; and (3) the concentration of mitochondrial markers in the experimental chamber are
 225 sample-specific normalizations, which are distinguished from system-specific normalization
 226 for the volume of the chamber (the measuring system).
- 227 6. The consistent use of terms and symbols will facilitate transdisciplinary communication and
 228 support the further development of a collaborative database on bioenergetics and
 229 mitochondrial physiology. The present considerations are focused on studies with
 230 mitochondrial preparations. These will be extended in a series of reports on pathway control
 231 of mitochondrial respiration, respiratory states in intact cells, and harmonization of
 232 experimental procedures.
 233

234 **Box 1: In brief – Mitochondria and Bioblasts**

235 *‘For the physiologist, mitochondria afforded the first opportunity for an experimental*
 236 *approach to structure-function relationships, in particular those involved in active*
 237 *transport, vectorial metabolism, and metabolic control mechanisms on a subcellular level’*
 238 *(Ernster and Schatz 1981).*

239 Mitochondria are oxygen-consuming electrochemical generators that evolved from the endosymbiotic
 240 alphaproteobacteria which integrated into a host cell related to Asgard Archaea (Margulis 1970; Lane
 241 2005; Roger *et al.* 2017). They were described by Richard Altmann (1894) as ‘bioblasts’, which include
 242 not only the mitochondria as presently defined, but also symbiotic and free-living bacteria. The word
 243 ‘mitochondria’ (Greek mitos: thread; chondros: granule) was introduced by Carl Benda (1898).

244 Contrary to current textbook dogma, mitochondria form dynamic networks within eukaryotic
 245 cells. Mitochondrial movement is supported by microtubules and morphology can change in response
 246 to energy requirements of the cell via processes known as fusion and fission; these interactions allow
 247 mitochondria to communicate within a network (Chan 2006). Mitochondria can even traverse cell
 248 boundaries in a process known as horizontal mitochondrial transfer (Torralba *et al.* 2016). Another
 249 defining characteristic of mitochondria is the double membrane. The mitochondrial inner membrane
 250 (mtIM) forms dynamic tubular to disk-shaped cristae that separate the mitochondrial matrix, *i.e.*, the
 251 negatively charged internal mitochondrial compartment, from the intermembrane space; the latter being
 252 enclosed by the mitochondrial outer membrane (mtOM) and positively charged with respect to the
 253 matrix. The mtIM contains the non-bilayer phospholipid cardiolipin, which is not present in any other
 254 eukaryotic cellular membrane. Cardiolipin has many regulatory functions (Oemer *et al.* 2018); in
 255 particular, it stabilizes and promotes the formation of respiratory supercomplexes (SC I_nIII_nIV_n), which
 256 are supramolecular assemblies based upon specific and dynamic interactions between individual
 257 respiratory complexes (Greggio *et al.* 2017; Lenaz *et al.* 2017). The fluidity of the mitochondrial
 258 membrane is plastic and exerts an influence on the functional properties of proteins incorporated in
 259 membranes (Waczulikova *et al.* 2007). Intracellular stress factors may cause shrinking or swelling of
 260 the mitochondrial matrix, that can ultimately result in permeability transition.

261 Mitochondria are the structural and functional elementary components of cell respiration.
 262 Mitochondrial respiration is the reduction of molecular oxygen by electron transfer coupled to
 263 electrochemical proton translocation across the mtIM. In the process of oxidative phosphorylation
 264 (OXPHOS), the catabolic reaction of oxygen consumption is electrochemically coupled to the
 265 transformation of energy in the form of adenosine triphosphate (ATP; Mitchell 1961, 2011).
 266 Mitochondria are the powerhouses of the cell which contain the machinery of the OXPHOS-pathways,
 267 including transmembrane respiratory complexes (proton pumps with FMN, Fe-S and cytochrome *b*, *c*,
 268 *aa*₃ redox systems); alternative dehydrogenases and oxidases; the coenzyme ubiquinone (Q); F-ATPase
 269 or ATP synthase; the enzymes of the tricarboxylic acid cycle (TCA), fatty acid and amino acid oxidation;
 270 transporters of ions, metabolites and co-factors; iron/sulphur cluster synthesis; and mitochondrial
 271 kinases related to energy transfer pathways. The mitochondrial proteome comprises over 1,200 proteins
 272 (Calvo *et al.* 2015; 2017), mostly encoded by nuclear DNA (nDNA), with a variety of functions, many
 273 of which are relatively well known (*e.g.*, proteins regulating mitochondrial biogenesis or apoptosis),
 274 while others are still under investigation, or need to be identified (*e.g.*, permeability transition pore,
 275 alanine transporter). Only recently has it been possible to use the mammalian mitochondrial proteome
 276 to discover and characterize the genetic basis of mitochondrial diseases (Williams *et al.* 2016; Palmfeldt
 277 and Bross 2017).

278 Numerous cellular processes are orchestrated by a constant crosstalk between mitochondria and
 279 other cellular components. For example, the crosstalk between mitochondria and the endoplasmic
 280 reticulum is involved in the regulation of calcium homeostasis, cell division, autophagy, differentiation,
 281 and anti-viral signaling (Murley and Nunnari 2016). Mitochondria contribute to the formation of
 282 peroxisomes, which are hybrids of mitochondrial and ER-derived precursors (Sugiura *et al.* 2017).
 283 Cellular mitochondrial homeostasis (mitostasis) is maintained through regulation at transcriptional,
 284 post-translational and epigenetic levels. Cell signalling modules contribute to homeostatic regulation
 285 throughout the cell cycle or even cell death by activating proteostatic modules (*e.g.*, the ubiquitin-
 286 proteasome and autophagy-lysosome/vacuole pathways; specific proteases like LON) and genome
 287 stability modules in response to varying energy demands and stress cues (Quiros *et al.* 2016). Several
 288 post-translational modifications, including acetylation and nitrosylation, are also capable of influencing
 289 the bioenergetic response, with clinically significant implications for health and disease (Carrico *et al.*
 290 2018).

291 Mitochondria of higher eukaryotes typically maintain several copies of their own circular genome
 292 known as mitochondrial DNA (mtDNA; hundred to thousands per cell; Cummins 1998), which is
 293 maternally inherited in humans. Biparental mitochondrial inheritance is documented in mammals, birds,
 294 fish, reptiles and invertebrate groups, and is even the norm in some bivalve taxonomic groups (Breton
 295 *et al.* 2007; White *et al.* 2008). The mitochondrial genome of the angiosperm *Amborella* contains a
 296 record of six mitochondrial genome equivalents acquired by horizontal transfer of entire genomes, two
 297 from angiosperms, three from algae and one from mosses (Rice *et al.* 2016). In unicellular organisms
 298 (*i.e.*, protists) the structural organization of mitochondrial genomes is highly variable and includes
 299 circular and linear DNA (Zikova *et al.* 2016). While some of the free-living flagellates exhibit the largest
 300 known gene coding capacity (*e.g.* jakobid *Andalucia godoyi* mitochondrial DNA codes for 106 genes)
 301 (Burger *et al.* 2013), some protist groups (*e.g.* alveolates) possess mitochondrial genomes encoding only
 302 three protein-coding genes and two rRNAs (Feagin *et al.* 2012). The complete loss of mitochondrial
 303 genome is observed in highly reduced mitochondria of *Cryptosporidium* species (Liu *et al.* 2016).
 304 Reaching the final extreme, the microbial eukaryote, oxymonad *Monocercomonoides*, has no
 305 mitochondrion whatsoever and lacks all typical nuclear-encoded mitochondrial proteins demonstrating
 306 that while in 99% of organisms mitochondria play a vital role, this organelle is not indispensable
 307 (Karnkowska *et al.* 2016).

308 In vertebrates but not all invertebrates, mtDNA is compact (16.5 kB in humans) and encodes 13
 309 protein subunits of the transmembrane respiratory Complexes CI, CIII, CIV and F-ATPase, 22 tRNAs,
 310 and two rRNAs. Additional gene content has been suggested to include microRNAs, piRNA,
 311 smithRNAs, repeat associated RNA, and even additional proteins (Duarte *et al.* 2014; Lee *et al.* 2015;
 312 Cobb *et al.* 2016). The mitochondrial genome requires nuclear-encoded mitochondrially targeted
 313 proteins, *e.g.*, TFAM, for its maintenance and expression (Rackham *et al.* 2012). Both genomes encode
 314 peptides of the membrane spanning redox pumps (CI, CIII and CIV) and F-ATPase, leading to strong
 315 constraints in the coevolution of both genomes (Blier *et al.* 2001).

316 Given the multiple roles of mitochondria, it is perhaps not surprising that mitochondrial
 317 dysfunction is associated with a wide variety of genetic and degenerative diseases. Robust mitochondrial
 318 function is supported by physical exercise and caloric balance, and is central for sustained metabolic
 319 health throughout life. Therefore, a more consistent set of definitions for mitochondrial physiology will
 320 increase our understanding of the etiology of disease and improve the diagnostic repertoire of
 321 mitochondrial medicine with a focus on protective medicine, lifestyle and healthy aging.

322 Mitochondrion is singular and mitochondria is plural. Abbreviation: mt, as generally used in
 323 mtDNA.

324

325

326

327

1. Introduction

328

329 Mitochondria are the powerhouses of the cell with numerous physiological, molecular, and
 330 genetic functions (**Box 1**). Every study of mitochondrial health and disease faces **Evolution, Age,**
 331 **Gender and sex, Lifestyle, and Environment (MitoEAGLE)** as essential background conditions intrinsic
 332 to the individual person or cohort, species, tissue and to some extent even cell line. As a large and
 333 coordinated group of laboratories and researchers, the mission of the global MitoEAGLE Network is to

334 generate the necessary scale, type, and quality of consistent data sets and conditions to address this
 335 intrinsic complexity. Harmonization of experimental protocols and implementation of a quality control
 336 and data management system are required to interrelate results gathered across a spectrum of studies
 337 and to generate a rigorously monitored database focused on mitochondrial respiratory function. In this
 338 way, researchers from a variety of disciplines can compare their findings using clearly defined and
 339 accepted international standards.

340 With an emphasis on quality of research, published data can be useful far beyond the specific
 341 question of a particular experiment. For example, collaborative data sets support the development of
 342 open-access databases such as those that have been developed for National Institutes of Health
 343 sponsored research in genetics, proteomics, and metabolomics. Indeed, enabling meta-analytic studies
 344 is the most economic way of providing robust answers to biological questions (Cooper *et al.* 2009).
 345 However, the reproducibility of quantitative results and databases depend on accurate measurements
 346 under strictly-defined conditions. Likewise, meaningful interpretation and comparability of
 347 experimental outcomes requires standardisation of protocols between research groups at different
 348 institutes. In addition to quality control, a conceptual framework is also required to standardise and
 349 homogenise terminology and methodology. Vague or ambiguous jargon can lead to confusion and may
 350 relegate valuable signals to wasteful noise. For this reason, measured values must be expressed in
 351 standard units for each parameter used to define mitochondrial respiratory function. Harmonization of
 352 nomenclature and definition of technical terms are essential to improve the awareness of the intricate
 353 meaning of current and past scientific vocabulary; this is important for documentation and integration
 354 into databases in general, and quantitative modelling in particular (Beard 2005).

355 In this review, we focus on coupling states and fluxes through metabolic pathways of aerobic
 356 energy transformation in mitochondrial preparations as a first step in the attempt to generate a
 357 conceptually-oriented nomenclature in bioenergetics and mitochondrial physiology. Respiratory control
 358 by fuel substrates and specific inhibitors of respiratory enzymes, coupling states of intact cells, and
 359 respiratory flux control ratios will be reviewed in subsequent communications, prepared in the frame of
 360 COST Action MitoEAGLE open to global bottom-up input.

361

362 **2. Coupling states and rates in mitochondrial preparations**

363 *‘Every professional group develops its own technical jargon for talking about matters of critical*
 364 *concern ... People who know a word can share that idea with other members of their group, and*
 365 *a shared vocabulary is part of the glue that holds people together and allows them to create a*
 366 *shared culture’* (Miller 1991).

367

368 *2.1. Cellular and mitochondrial respiration*

369

370 **2.1.1. Aerobic and anaerobic catabolism and ATP turnover:** In respiration, electron transfer
 371 is coupled to the phosphorylation of ADP to ATP, with energy transformation mediated by the
 372 protonmotive force, Δp (**Figure 2**). Anabolic reactions are coupled to catabolism, both by ATP as the
 373 intermediary energy currency and by small organic precursor molecules as building blocks for
 374 biosynthesis. Glycolysis involves substrate-level phosphorylation of ADP to ATP in fermentation
 375 without utilization of O₂, studied mainly in intact cells and organisms. Many cellular fuel substrates are
 376 catabolized to acetyl-CoA or to glutamate, and further electron transfer reduces nicotinamide adenine
 377 dinucleotide to NADH or flavin adenine dinucleotide to FADH₂. Subsequent mitochondrial electron
 378 transfer to O₂ is coupled to proton translocation for the control of Δp and phosphorylation of ADP
 379 (**Figure 2B and 2C**). In contrast, extra-mitochondrial oxidation of fatty acids and amino acids proceeds
 380 partially in peroxisomes without coupling to ATP production: acyl-CoA oxidase catalyzes the oxidation
 381 of FADH₂ with electron transfer to O₂; amino acid oxidases oxidize flavin mononucleotide FMNH₂ or
 382 FADH₂ (**Figure 2A**).

383 The plasma membrane separates the intracellular compartment including the cytosol, nucleus, and
 384 organelles from the extracellular environment. The plasma membrane consists of a lipid bilayer with
 385 embedded proteins and attached organic molecules that collectively control the selective permeability
 386 of ions, organic molecules, and particles across the cell boundary. The intact plasma membrane prevents
 387 the passage of many water-soluble mitochondrial substrates and inorganic ions—such as succinate,
 388 adenosine diphosphate (ADP) and inorganic phosphate (P_i), that must be precisely controlled at
 389 kinetically-saturating concentrations for the analysis of mitochondrial respiratory capacities.

390 Respiratory capacities delineate, comparable to channel capacity in information theory (Schneider
 391 2006), the upper bound of the rate of O₂ consumption measured in defined respiratory states. Despite
 392 the activity of solute carriers, *e.g.*, SLC13A3 and SLC20A2, which transport specific metabolites across
 393 the plasma membrane of various cell types, the intact plasma membrane limits the scope of
 394 investigations into mitochondrial respiratory function in intact cells.

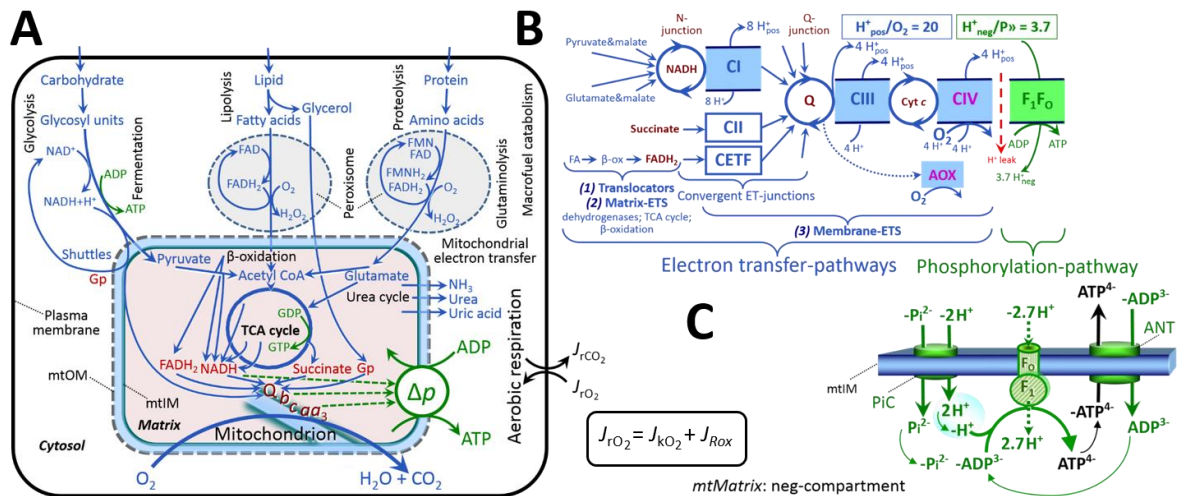
395 **2.1.2. Specification of biochemical dose:** Substrates, uncouplers, inhibitors, and other chemical
 396 reagents are titrated to analyse cellular and mitochondrial function. Nominal concentrations of these
 397 substances are usually reported as initial amount of substance concentration [mol·L⁻¹] in the incubation
 398 medium. When aiming at the measurement of kinetically saturated processes—such as OXPPOS-
 399 capacities, the concentrations for substrates can be chosen according to the apparent equilibrium
 400 constant, K_m' . In the case of hyperbolic kinetics, only 80% of maximum respiratory capacity is obtained
 401 at a substrate concentration of four times the K_m' , whereas substrate concentrations of 5, 9, 19 and 49
 402 times the K_m' are theoretically required for reaching 83%, 90%, 95% or 98% of the maximal rate
 403 (Gnaiger 2001). Other reagents are chosen to inhibit or alter a particular process. The amount of these
 404 chemicals in an experimental incubation is selected to maximize effect, avoiding unacceptable off-target
 405 consequences that would adversely affect the data being sought. Specifying the amount of substance in
 406 an incubation as nominal concentration in the aqueous incubation medium can be ambiguous (Doskey
 407 *et al.* 2015), particularly for cations (TPP⁺; fluorescent dyes such as safranin, TMRM; Chowdhury *et al.*
 408 2015) and lipophilic substances (oligomycin, uncouplers, permeabilization agents; Doerrier *et al.* 2018),
 409 which accumulate in the mitochondrial matrix or in biological membranes, respectively. Generally,
 410 dose/exposure can be specified per unit of biological sample, *i.e.*, (nominal moles of
 411 xenobiotic)/(number of cells) [mol·cell⁻¹] or, as appropriate, per mass of biological sample [mol·kg⁻¹].
 412 This approach to specification of dose/exposure provides a scalable parameter that can be used to design
 413 experiments, help interpret a wide variety of experimental results, and provide absolute information that
 414 allows researchers worldwide to make the most use of published data (Doskey *et al.* 2015).
 415

416 2.2. Mitochondrial preparations

417
 418 Mitochondrial preparations are defined as either isolated mitochondria, or tissue and cellular
 419 preparations in which the barrier function of the plasma membrane is disrupted. Since this entails the
 420 loss of cell viability, mitochondrial preparations are not studied *in vivo*. In contrast to isolated
 421 mitochondria and tissue homogenate preparations, mitochondria in permeabilized tissues and cells are
 422 *in situ* relative to the plasma membrane. When studying mitochondrial preparations, substrate-
 423 uncoupler-inhibitor-titration (SUIT) protocols can be used to establish respiratory coupling control
 424 states (CCS) and pathway control states (PCS) that provide reference values for various output variables
 425 (**Table 1**). Physiological conditions *in vivo* deviate from these experimentally obtained states; this is
 426 because kinetically-saturating concentrations, *e.g.*, of ADP, oxygen (O₂; dioxygen) or fuel substrates,
 427 may not apply to physiological intracellular conditions. Further information is obtained in studies of
 428 kinetic responses to variations in fuel substrate concentrations, [ADP], or [O₂] in the range between
 429 kinetically-saturating concentrations and anoxia (Gnaiger 2001).
 430

431 The cholesterol content of the plasma membrane is high compared to mitochondrial membranes
 432 (Korn 1969). Therefore, mild detergents—such as digitonin and saponin—can be applied to selectively
 433 permeabilize the plasma membrane via interaction with cholesterol; this allows free exchange of organic
 434 molecules and inorganic ions between the cytosol and the immediate cell environment, while
 435 maintaining the integrity and localization of organelles, cytoskeleton, and the nucleus. Application of
 436 permeabilization agents (mild detergents or toxins) leads to washout of cytosolic marker enzymes—
 437 such as lactate dehydrogenase—and results in the complete loss of cell viability (tested by nuclear
 438 staining using plasma membrane-impermeable dyes), while mitochondrial function remains intact
 439 (tested by cytochrome *c* stimulation of respiration). Digitonin concentrations have to be optimized
 440 according to cell type, particularly since mitochondria from cancer cells contain significantly higher
 441 contents of cholesterol in both membranes (Baggetto and Testa-Perussini, 1990). For example, a dose
 442 of digitonin of 8 fmol·cell⁻¹ (10 pg·cell⁻¹; 10 μg·10⁻⁶ cells) is optimal for permeabilization of endothelial
 443 cells, and the concentration in the incubation medium has to be adjusted according to the cell density
 444 applied (Doerrier *et al.* 2018). Respiration of isolated mitochondria remains unaltered after the addition
 of low concentrations of digitonin or saponin. In addition to mechanical cell disruption during

445 homogenization of tissue, permeabilization agents may be applied to ensure permeabilization of all cells
 446 in tissue homogenates.
 447



448 **Figure 2. Cell respiration and oxidative phosphorylation (OXPHOS)**
 449 Mitochondrial respiration is the oxidation of fuel substrates (electron donors) with electron transfer to
 450 O_2 as the electron acceptor. For explanation of symbols see also **Figure 1**.

451 **(A)** Respiration of intact cells: Extra-mitochondrial catabolism of macrofuels and uptake of small
 452 molecules by the cell provide the mitochondrial fuel substrates. Dashed arrows indicate the connection
 453 between the redox proton pumps (respiratory Complexes CI, CIII and CIV) and the transmembrane Δp .
 454 Coenzyme Q (Q) and the cytochromes *b*, *c*, and *aa*₃ are redox systems of the mitochondrial inner
 455 membrane, mtIM. Glycerol-3-phosphate, Gp.

456 **(B)** Respiration in mitochondrial preparations: The mitochondrial electron transfer system (ETS) is (1)
 457 fuelled by diffusion and transport of substrates across the mtOM and mtIM, and in addition consists of
 458 the (2) matrix-ETS, and (3) membrane-ETS. Electron transfer converges at the N-junction, and from CI,
 459 CII and electron transferring flavoprotein complex (CETF) at the Q-junction. Unspecified arrows
 460 converging at the Q-junction indicate additional ET-sections with electron entry into Q through
 461 glycerophosphate dehydrogenase, dihydro-orotate dehydrogenase, proline dehydrogenase, choline
 462 dehydrogenase, and sulfide-ubiquinone oxidoreductase. The dotted arrow indicates the branched
 463 pathway of oxygen consumption by alternative quinol oxidase (AOX). ET-pathways are coupled to the
 464 phosphorylation-pathway. The $\text{H}^+_{\text{pos}}/\text{O}_2$ ratio is the outward proton flux from the matrix space to the
 465 positively (pos) charged vesicular compartment, divided by catabolic O_2 flux in the NADH-pathway.
 466 The $\text{H}^+_{\text{neg}}/\text{P}$ ratio is the inward proton flux from the inter-membrane space to the negatively (neg)
 467 charged matrix space, divided by the flux of phosphorylation of ADP to ATP. These stoichiometries are
 468 not fixed due to ion leaks and proton slip. Modified from (B) Lemieux *et al.* (2017) and Rich (2013).

469 **(C)** Chemiosmotic phosphorylation-pathway catalyzed by the proton pump F_1F_0 -ATPase (F-ATPase,
 470 ATP synthase), adenine nucleotide translocase (ANT), and inorganic phosphate carrier (PiC). The
 471 $\text{H}^+_{\text{neg}}/\text{P}$ stoichiometry is the sum of the coupling stoichiometry in the F-ATPase reaction ($-2.7 \text{H}^+_{\text{pos}}$
 472 from the positive intermembrane space, $2.7 \text{H}^+_{\text{neg}}$ to the matrix, *i.e.*, the negative compartment) and the
 473 proton balance in the translocation of ADP^{3-} , ATP^{4-} and P_i^{2-} . Modified from Gnaiger (2014).
 474
 475

476 Suspensions of cells permeabilized in the respiration chamber and crude tissue homogenates
 477 contain all components of the cell at highly dilute concentrations. All mitochondria are retained in
 478 chemically-permeabilized mitochondrial preparations and crude tissue homogenates. In the preparation
 479 of isolated mitochondria, however, the mitochondria are separated from other cell fractions and purified
 480 by differential centrifugation, entailing the loss of mitochondria at typical recoveries ranging from 30%
 481 to 80% of total mitochondrial content (Lai *et al.* 2018). Using Percoll or sucrose density gradients to
 482 maximize the purity of isolated mitochondria may compromise the mitochondrial yield or structural and
 483 functional integrity. Therefore, mitochondrial isolation protocols need to be optimized according to each
 484 study. The term mitochondrial preparation does neither include intact cells, nor submitochondrial
 485 particles and further fractionation of mitochondrial components.

486 2.3. Electron transfer pathways

487
488 Mitochondrial electron transfer (ET) pathways are fuelled by diffusion and transport of substrates
489 across the mtOM and mtIM. In addition, the mitochondrial electron transfer system (ETS) consists of
490 the matrix-ETS, and membrane-ETS (**Figure 2B**). Upstream sections of ET-pathways converge at the
491 NADH-junction (N-junction). NADH is mainly generated in the tricarboxylic acid (TCA) cycle and is
492 oxidized by Complex I (CI), with further electron entry into the coenzyme Q-junction (Q-junction).
493 Similarly, succinate is formed in the TCA cycle and oxidized by CII to fumarate. CII is part of both the
494 TCA cycle and the ETS, and reduces FAD to FADH₂ with further reduction of ubiquinone to ubiquinol
495 downstream of the TCA cycle in the Q-junction. Thus FADH₂ is not a substrate but is the product of
496 CII, in contrast to erroneous metabolic maps shown in many publications. β -oxidation of fatty acids
497 (FA) generates FADH₂ as the substrate of electron transferring flavoprotein complex (CETF).

498 Selected mitochondrial catabolic pathways, k, of electron transfer from the oxidation of fuel
499 substrates to the reduction of O₂ are activated by depletion of endogenous substrates and addition of fuel
500 substrates to the mitochondrial respiration medium (**Figure 2B**; 2[H] in **Figure 3**). Substrate
501 combinations and specific inhibitors of ET-pathway enzymes are used to obtain defined pathway control
502 states in mitochondrial preparations (Gnaiger 2014).

503 504 2.4. Respiratory coupling control

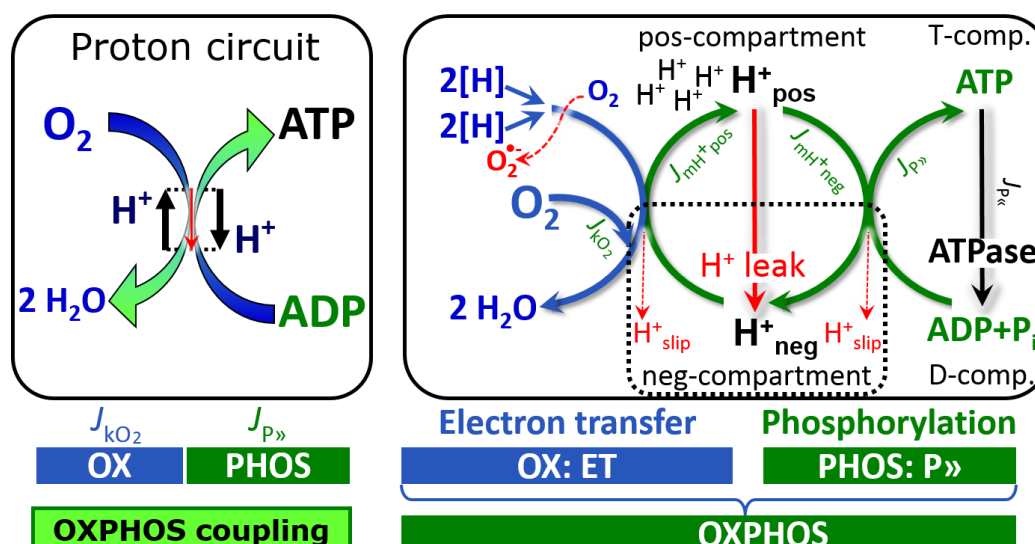
505
506 **2.4.1. Coupling:** In mitochondrial electron transfer, vectorial transmembrane proton flux is
507 coupled through the redox proton pumps CI, CIII and CIV to the catabolic flux of scalar reactions,
508 collectively measured as O₂ flux (**Figure 3**). Thus mitochondria are elementary components of energy
509 transformation. Energy is a conserved quantity and cannot be lost or produced in any internal process
510 (First Law of thermodynamics). Open and closed systems can gain or lose energy only by external
511 fluxes—by exchange with the environment. Therefore, energy can neither be produced by mitochondria,
512 nor is there any internal process without energy conservation. Exergy or Gibbs energy (‘free energy’) is
513 the part of energy that can potentially be transformed into work under conditions of constant temperature
514 and pressure. *Coupling* is the interaction of an exergonic process (spontaneous, negative exergy change)
515 with an endergonic process (positive exergy change) in energy transformations which conserve part of
516 the exergy that would be irreversibly lost or dissipated in an uncoupled process.

517 Pathway control states (PCS) and coupling control states (CCS) are complementary, since
518 mitochondrial preparations depend on (1) an exogenous supply of pathway-specific fuel substrates and
519 oxygen, and (2) exogenous control of phosphorylation (**Figure 2**).

520 **2.4.2. Phosphorylation, P_», and P_»/O₂ ratio:** *Phosphorylation* in the context of OXPHOS is
521 defined as phosphorylation of ADP by P_i to form ATP. On the other hand, the term phosphorylation is
522 used generally in many contexts, *e.g.*, protein phosphorylation. This justifies consideration of a symbol
523 more discriminating and specific than P as used in the P/O ratio (phosphate to atomic oxygen ratio),
524 where P indicates phosphorylation of ADP to ATP or GDP to GTP (**Figure 2**). We propose the symbol
525 P_» for the endergonic (uphill) direction of phosphorylation ADP→ATP, and likewise the symbol P_« for
526 the corresponding exergonic (downhill) hydrolysis ATP→ADP (**Figure 3**). P_» refers mainly to
527 electrontransfer phosphorylation but may also involve substrate-level phosphorylation as part of the
528 TCA cycle (succinyl-CoA ligase; phosphoglycerate kinase) and phosphorylation of ADP catalyzed by
529 pyruvate kinase, and of GDP phosphorylated by phosphoenolpyruvate carboxykinase.
530 Transphosphorylation is performed by adenylate kinase, creatine kinase (mtCK), hexokinase and
531 nucleoside diphosphate kinase. In isolated mammalian mitochondria, ATP production catalyzed by
532 adenylate kinase (2 ADP ↔ ATP + AMP) proceeds without fuel substrates in the presence of ADP
533 (Kömłódi and Tretter 2017). Kinase cycles are involved in intracellular energy transfer and signal
534 transduction for regulation of energy flux.

535

536



537 **Figure 3. Coupling in oxidative phosphorylation (OXPHOS)**
 538 $2[H]$ indicates the reduced hydrogen equivalents of fuel substrates of the catabolic reaction k with 0.5
 539 O_2 . O_2 flux, J_{kO_2} , through the catabolic ET-pathway, is coupled to flux through the phosphorylation-
 540 pathway of ADP to ATP, $J_{P\gg}$. The redox proton pumps of the ET-pathway drive proton flux into the
 541 positive (pos) compartment, J_{mH^+pos} , generating the output protonmotive force (motive, subscript m). F-
 542 ATPase is coupled to inward proton current into the negative (neg) compartment, J_{mH^+neg} , to
 543 phosphorylate ADP to ATP. The system is defined by the boundaries (full black line) and is not a black
 544 box, but is analysed as a compartmental system. The negative compartment (neg-compartment,
 545 enclosed by the dotted line) is the matrix space, separated by the mtIM from the positive compartment
 546 (pos-compartment). ADP+ P_i and ATP are the substrate- and product-compartments (scalar ADP and
 547 ATP compartments, D-comp. and T-comp.), respectively. At steady-state proton turnover, $J_{\infty H^+}$, and
 548 ATP turnover, $J_{\infty P\gg}$, maintain concentrations constant, when $J_{mH^+\infty} = J_{mH^+pos} = J_{mH^+neg}$, and $J_{P\gg} = J_{P\gg} = J_{P\ll}$.
 549 Modified from Gnaiger (2014).

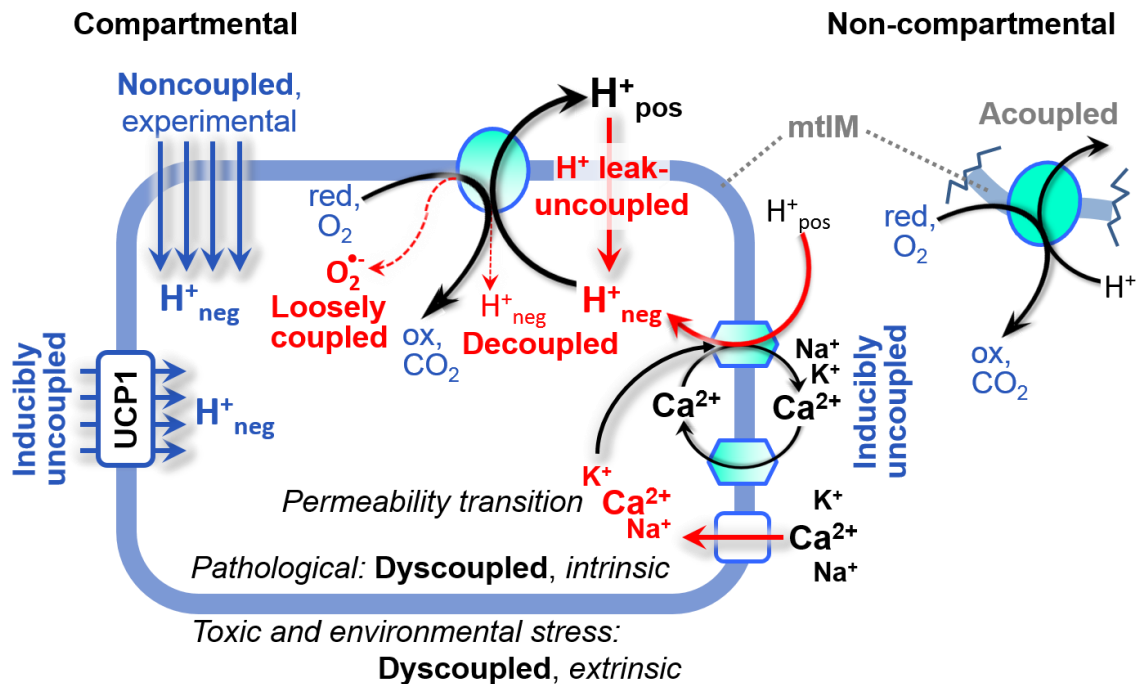
550
 551 The $P\gg/O_2$ ratio ($P\gg/4 e^-$) is two times the ‘P/O’ ratio ($P\gg/2 e^-$) of classical bioenergetics. $P\gg/O_2$
 552 is a generalized symbol, not specific for determination of P_i consumption (P_i/O_2 flux ratio), ADP depletion
 553 (ADP/O_2 flux ratio), or ATP production (ATP/O_2 flux ratio). The mechanistic $P\gg/O_2$ ratio—or $P\gg/O_2$
 554 stoichiometry—is calculated from the proton-to- O_2 and proton-to-phosphorylation coupling
 555 stoichiometries (**Figure 2B**):

556
 557
$$P\gg/O_2 = \frac{H_{pos}^+/O_2}{H_{neg}^+/P\gg} \quad (1)$$

558
 559 The H_{pos}^+/O_2 coupling stoichiometry (referring to the full 4 electron reduction of O_2) depends on the
 560 relative involvement of the three coupling sites (respiratory Complexes CI, CIII and CIV) in the
 561 catabolic ET-pathway from reduced fuel substrates (electron donors) to the reduction of O_2 (electron
 562 acceptor). This varies with: (1) a bypass of CI by single or multiple electron input into the Q-junction;
 563 and (2) a bypass of CIV by involvement of alternative oxidases, AOX, which are not expressed in
 564 mammalian mitochondria.

565 The H_{pos}^+/O_2 coupling stoichiometry equals 12 in the ET-pathways involving CIII and CIV as
 566 proton pumps, increasing to 20 for the NADH-pathway through CI (**Figure 2B**), but a general consensus
 567 on H_{pos}^+/O_2 stoichiometries remains to be reached (Hinkle 2005; Wikström and Hummer 2012; Sazanov
 568 2015). The $H_{neg}^+/P\gg$ coupling stoichiometry (3.7; **Figure 2B**) is the sum of 2.7 H_{neg}^+ required by the F-
 569 ATPase of vertebrate and most invertebrate species (Watt *et al.* 2010) and the proton balance in the
 570 translocation of ADP, ATP and P_i (**Figure 2C**). Taken together, the mechanistic $P\gg/O_2$ ratio is calculated
 571 at 5.4 and 3.3 for NADH- and succinate-linked respiration, respectively (Eq. 1). The corresponding
 572 classical $P\gg/O$ ratios (referring to the 2 electron reduction of $0.5 O_2$) are 2.7 and 1.6 (Watt *et al.* 2010),
 573 in agreement with the measured $P\gg/O$ ratio for succinate of 1.58 ± 0.02 (Gnaiger *et al.* 2000).

574 **2.4.3. Uncoupling:** The effective P_{O_2} flux ratio ($Y_{P_{\text{O}_2}} = J_{P_{\text{O}_2}}/J_{\text{K}_{\text{O}_2}}$; **Figure 3**) is diminished
 575 relative to the mechanistic P_{O_2} ratio by intrinsic and extrinsic uncoupling or dyscoupling (**Figure 4**).
 576 Such generalized uncoupling is different from switching to mitochondrial pathways that involve fewer
 577 than three proton pumps ('coupling sites': Complexes CI, CIII and CIV), bypassing CI through multiple
 578 electron entries into the Q-junction, or CIII and CIV through AOX (**Figure 2B**). Reprogramming of
 579 mitochondrial pathways leading to different types of substrates being oxidized may be considered as a
 580 switch of gears (changing the stoichiometry by altering the substrate that is oxidized) rather than
 581 uncoupling (loosening the tightness of coupling relative to a fixed stoichiometry). In addition, $Y_{P_{\text{O}_2}}$
 582 depends on several experimental conditions of flux control, increasing as a hyperbolic function of [ADP]
 583 to a maximum value (Gnaiger 2001).
 584



585 **Figure 4. Mechanisms of respiratory uncoupling**

586 An intact mitochondrial inner membrane, mtIM, is required for vectorial, compartmental coupling.
 587 'Acoupled' respiration is the consequence of structural disruption with catalytic activity of non-
 588 compartmental mitochondrial fragments. Inducibly uncoupled (activation of UCP1) and experimentally
 589 noncoupled respiration (titration of protonophores) stimulate respiration to maximum O₂ flux. H⁺ leak-
 590 uncoupled, decoupled, and loosely coupled respiration are components of intrinsic uncoupling (**Table**
 591 **2**). Pathological dysfunction may affect all types of uncoupling, including permeability transition,
 592 causing intrinsically dyscoupled respiration. Similarly, toxicological and environmental stress factors
 593 can cause extrinsically dyscoupled respiration. Reduced fuel substrates, red; oxidized products, ox.
 594

595 Uncoupling of mitochondrial respiration is a general term comprising diverse mechanisms:

- 596 1. Proton leak across the mtIM from the pos- to the neg-compartment (H⁺ leak-uncoupled; **Figure**
 597 **4**).
- 598 2. Cycling of other cations, strongly stimulated by permeability transition; comparable to the use of
 599 protonophores, cation cycling is experimentally induced by valinomycin in the presence of K⁺;
- 600 3. Decoupling by proton slip in the redox proton pumps when protons are effectively not pumped
 601 (CI, CIII and CIV) or are not driving phosphorylation (F-ATPase);
- 602 4. Loss of vesicular (compartmental) integrity when electron transfer is acoupled;
- 603 5. Electron leak in the loosely coupled univalent reduction of O₂ to superoxide (O₂^{•-}; superoxide
 604 anion radical).

605 Differences of terms—uncoupled vs. noncoupled—are easily overlooked, although they relate to
 606 different meanings of uncoupling (**Figure 4** and **Table 2**).

607
 608

609 2.5. Coupling states and respiratory rates

610

611 To extend the classical nomenclature on mitochondrial coupling states (Section 2.6) by a concept-
 612 driven terminology that explicitly incorporates information on the meaning of respiratory states, the
 613 terminology must be general and not restricted to any particular experimental protocol or mitochondrial
 614 preparation (Gnaiger 2009). Concept-driven nomenclature aims at mapping the *meaning and concept*
 615 *behind* the words and acronyms onto the *forms* of words and acronyms (Miller 1991). The focus of
 616 concept-driven nomenclature is primarily the conceptual *why*, along with clarification of the
 617 experimental *how*.

618

619 **Table 1. Coupling states and residual oxygen consumption in mitochondrial**
 620 **preparations in relation to respiration- and phosphorylation-flux, J_{KO_2} and J_{P} , and**
 621 **protonmotive force, Δp .** Coupling states are established at kinetically-saturating
 622 concentrations of fuel substrates and O_2 .

State	J_{KO_2}	J_{P}	Δp	Inducing factors	Limiting factors
LEAK	L ; low, cation leak-dependent respiration	0	max.	back-flux of cations including proton leak, proton slip	$J_{\text{P}} = 0$: (1) without ADP, L_N ; (2) max. ATP/ADP ratio, L_T ; or (3) inhibition of the phosphorylation-pathway, L_{omy}
OXPHOS	P ; high, ADP-stimulated respiration	max.	high	kinetically-saturating [ADP] and $[\text{P}_i]$	J_{P} by phosphorylation-pathway; or J_{KO_2} by ET-capacity
ET	E ; max., noncoupled respiration	0	low	optimal external uncoupler concentration for max. $J_{\text{O}_2, E}$	J_{KO_2} by ET-capacity
ROX	R_{ox} ; min., residual O_2 consumption	0	0	$J_{\text{O}_2, R_{\text{ox}}}$ in non-ET-pathway oxidation reactions	inhibition of all ET-pathways; or absence of fuel substrates

623

624

625 To provide a diagnostic reference for respiratory capacities of core energy metabolism, the
 626 capacity of *oxidative phosphorylation*, OXPHOS, is measured at kinetically-saturating concentrations
 627 of ADP and P_i . The *oxidative* ET-capacity reveals the limitation of OXPHOS-capacity mediated by the
 628 *phosphorylation*-pathway. The ET- and phosphorylation-pathways comprise coupled segments of the
 629 OXPHOS-system. ET-capacity is measured as noncoupled respiration by application of *external*
 630 *uncouplers*. The contribution of *intrinsically uncoupled* O_2 consumption is studied by preventing the
 631 stimulation of phosphorylation either in the absence of ADP or by inhibition of the phosphorylation-
 632 pathway. The corresponding states are collectively classified as LEAK-states, when O_2 consumption
 633 compensates mainly for ion leaks, including the proton leak. Defined coupling states are induced by: (1)
 634 adding cation chelators such as EGTA, binding free Ca^{2+} and thus limiting cation cycling; (2) adding
 635 ADP and P_i ; (3) inhibiting the phosphorylation-pathway; and (4) uncoupler titrations, while maintaining
 636 a defined ET-pathway state with constant fuel substrates and inhibitors of specific branches of the ET-
 637 pathway.

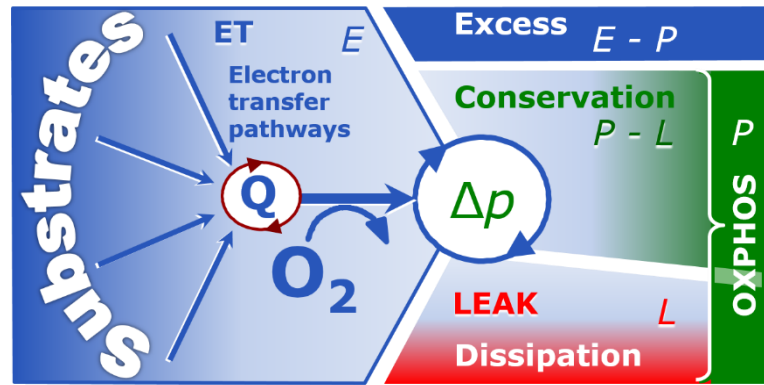
637

638

639 The three coupling states, ET, LEAK and OXPHOS, are shown schematically with the
 640 corresponding respiratory rates, abbreviated as E , L and P , respectively (**Figure 5**). We distinguish
 641 metabolic *pathways* from metabolic *states* and the corresponding metabolic *rates*; for example: ET-
 642 pathways, ET-states, and ET-capacities, E , respectively (**Table 1**). The protonmotive force is *high* in
 643 the OXPHOS-state when it drives phosphorylation, *maximum* in the LEAK-state of coupled
 mitochondria, driven by LEAK-respiration at a minimum back-flux of cations to the matrix side, and
very low in the ET-state when uncouplers short-circuit the proton cycle (**Table 1**).

644 **Figure 5. Four-compartment**
 645 **model of oxidative**
 646 **phosphorylation**

647 Respiratory states (ET, OXPHOS,
 648 LEAK; Table 1) and corresponding
 649 rates (E , P , L) are connected by the
 650 protonmotive force, Δp . (1) ET-
 651 capacity, E , is partitioned into (2)
 652 dissipative LEAK-respiration, L ,
 653 when the Gibbs energy change of
 654 catabolic O_2 flux is irreversibly lost,
 655 (3) net OXPHOS-capacity, $P-L$, with
 656 partial conservation of the capacity to
 657 perform work, and (4) the excess capacity,
 658 $E-P$. Modified from Gnaiger (2014).

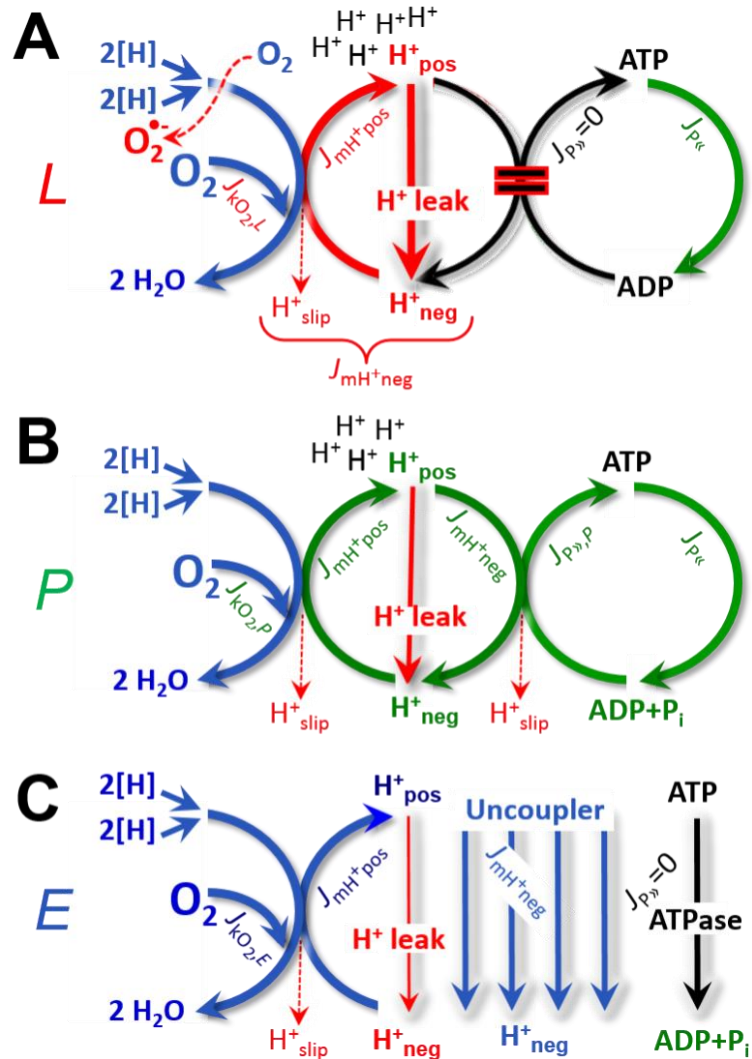


659 **Figure 6. Respiratory coupling**
 660 **states**

661 (A) **LEAK-state and rate, L** :
 662 Phosphorylation is arrested, $J_{P\gg} = 0$,
 663 and catabolic O_2 flux, $J_{kO_2,L}$, is
 664 controlled mainly by the proton
 665 leak, $J_{mH^{+neg},L}$, at maximum
 666 protonmotive force (Figure 4).
 667 Extramitochondrial ATP may be
 668 hydrolyzed by extramitochondrial
 669 ATPases, $J_{P\ll}$.

661 (B) **OXPHOS-state and rate, P** :
 662 Phosphorylation, $J_{P\gg}$, is stimulated
 663 by kinetically-saturating [ADP]
 664 and [P_i], and is supported by a high
 665 protonmotive force. O_2 flux, $J_{kO_2,P}$,
 666 is well-coupled at a $P\gg/O_2$ ratio of
 667 $J_{P\gg,P}/J_{O_2,P}$. Extramitochondrial
 668 ATPases may recycle ATP, $J_{P\ll}$.

661 (C) **ET-state and rate, E** :
 662 Noncoupled respiration, $J_{kO_2,E}$, is
 663 maximum at optimum exogenous
 664 uncoupler concentration and
 665 phosphorylation is zero, $J_{P\gg} = 0$.
 666 The F-ATPase may hydrolyze
 667 extramitochondrial ATP. See also
 668 Figure 3.



659
 660

661 **2.5.1. LEAK-state (Figure 6A):** The LEAK-state is defined as a state of mitochondrial
 662 respiration when O_2 flux mainly compensates for ion leaks in the absence of ATP synthesis, at
 663 kinetically-saturating concentrations of O_2 , respiratory fuel substrates and P_i . LEAK-respiration is
 664 measured to obtain an estimate of *intrinsic uncoupling* without addition of an experimental uncoupler:
 665 (1) in the absence of adenylates, *i.e.*, AMP, ADP and ATP; (2) after depletion of ADP at a maximum
 666 ATP/ADP ratio; or (3) after inhibition of the phosphorylation-pathway by inhibitors of F-ATPase—such
 667 as oligomycin, or of adenine nucleotide translocase—such as carboxyatractylsido. Adjustment of the

668 nominal concentration of these inhibitors to the density of biological sample applied can minimize or
 669 avoid inhibitory side-effects exerted on ET-capacity or even some dyscoupling.

- 670 • **Proton leak and uncoupled respiration:** The intrinsic proton leak is the *uncoupled* leak current
 671 of protons in which protons diffuse across the mtIM in the dissipative direction of the downhill
 672 protonmotive force without coupling to phosphorylation (**Figure 6A**). The proton leak flux
 673 depends non-linearly on the protonmotive force (Garlid *et al.* 1989; Divakaruni and Brand 2011),
 674 which is a temperature-dependent property of the mtIM and may be enhanced due to possible
 675 contaminations by free fatty acids. Inducible uncoupling mediated by uncoupling protein 1
 676 (UCP1) is physiologically controlled, *e.g.*, in brown adipose tissue. UCP1 is a member of the
 677 mitochondrial carrier family that is involved in the translocation of protons across the mtIM
 678 (Klingenberg 2017). Consequently, this short-circuit lowers the protonmotive force and
 679 stimulates electron transfer, respiration, and heat dissipation in the absence of phosphorylation of
 680 ADP.
- 681 • **Cation cycling:** There can be other cation contributors to leak current including calcium and
 682 probably magnesium. Calcium influx is balanced by mitochondrial $\text{Na}^+/\text{Ca}^{2+}$ or $\text{H}^+/\text{Ca}^{2+}$
 683 exchange, which is balanced by Na^+/H^+ or K^+/H^+ exchanges. This is another effective uncoupling
 684 mechanism different from proton leak (**Table 2**).
 685
 686

Table 2. Terms on respiratory coupling and uncoupling.

Term	J_{kO_2}	$P \gg O_2$	Notes	
acoupled		0	electron transfer in mitochondrial fragments without vectorial proton translocation (Figure 4)	
intrinsic, no protonophore added	uncoupled	L	0	non-phosphorylating LEAK-respiration (Figure 6A)
	proton leak-uncoupled		0	component of L , H^+ diffusion across the mtIM (Figure 4)
	decoupled		0	component of L , proton slip (Figure 4)
	loosely coupled		0	component of L , lower coupling due to superoxide formation and bypass of proton pumps by electron leak (Figure 4)
	dyscoupled		0	pathologically, toxicologically, environmentally increased uncoupling, mitochondrial dysfunction
	inducibly uncoupled		0	by UCP1 or cation (<i>e.g.</i> , Ca^{2+}) cycling (Figure 4)
noncoupled	E	0	ET-capacity, non-phosphorylating respiration stimulated to maximum flux at optimum exogenous uncoupler concentration (Figure 6C)	
well-coupled	P	high	OXPHOS-capacity , phosphorylating respiration with an intrinsic LEAK component (Figure 6B)	
fully coupled	$P - L$	max.	OXPHOS-capacity corrected for LEAK-respiration (Figure 5)	

- 687 • **Proton slip and decoupled respiration:** Proton slip is the *decoupled* process in which protons
 688 are only partially translocated by a redox proton pump of the ET-pathways and slip back to the
 689 original vesicular compartment. The proton leak is the dominant contributor to the overall leak
 690 current in mammalian mitochondria incubated under physiological conditions at 37 °C, whereas
 691 proton slip increases at lower experimental temperature (Canton *et al.* 1995). Proton slip can also
 692 happen in association with the F-ATPase, in which the proton slips downhill across the pump to
 693 the matrix without contributing to ATP synthesis. In each case, proton slip is a property of the
 694 proton pump and increases with the pump turnover rate.
- 695 • **Electron leak and loosely coupled respiration:** Superoxide production by the ETS leads to a
 696 bypass of redox proton pumps and correspondingly lower $P \gg O_2$ ratio. This depends on the actual
 697

698 site of electron leak and the scavenging of hydrogen peroxide by cytochrome *c*, whereby electrons
699 may re-enter the ETS with proton translocation by CIV.

- 700 • **Loss of compartmental integrity and acoupled respiration:** Electron transfer and catabolic O₂
701 flux proceed without compartmental proton translocation in disrupted mitochondrial fragments.
702 Such fragments are an artefact of mitochondrial isolation, and may not fully fuse to re-establish
703 structurally intact mitochondria. Loss of mtIM integrity, therefore, is the cause of acoupled
704 respiration, which is a nonvectorial dissipative process without control by the protonmotive force.
- 705 • **Dyscoupled respiration:** Mitochondrial injuries may lead to *dyscoupling* as a pathological or
706 toxicological cause of *uncoupled* respiration. Dyscoupling may involve any type of uncoupling
707 mechanism, *e.g.*, opening the permeability transition pore. Dyscoupled respiration is
708 distinguished from the experimentally induced *noncoupled* respiration in the ET-state (**Table 2**).
709

710 **2.5.2. OXPHOS-state (Figure 6B):** The OXPHOS-state is defined as the respiratory state with
711 kinetically-saturating concentrations of O₂, respiratory and phosphorylation substrates, and absence of
712 exogenous uncoupler, which provides an estimate of the maximal respiratory capacity in the OXPHOS-
713 state for any given ET-pathway state. Respiratory capacities at kinetically-saturating substrate
714 concentrations provide reference values or upper limits of performance, aiming at the generation of data
715 sets for comparative purposes. Physiological activities and effects of substrate kinetics can be evaluated
716 relative to the OXPHOS-capacity.

717 As discussed previously, 0.2 mM ADP does not fully saturate flux in isolated mitochondria
718 (Gnaiger 2001; Puchowicz *et al.* 2004); greater [ADP] is required, particularly in permeabilized muscle
719 fibres and cardiomyocytes, to overcome limitations by intracellular diffusion and by the reduced
720 conductance of the mtOM (Jepihhina *et al.* 2011, Illaste *et al.* 2012, Simson *et al.* 2016), either through
721 interaction with tubulin (Rostovtseva *et al.* 2008) or other intracellular structures (Birkedal *et al.* 2014).
722 In addition, saturating ADP concentrations need to be evaluated under different experimental conditions
723 such as temperature (Lemieux *et al.* 2017) and with different animal models (Blier and Guderley, 1993).
724 In permeabilized muscle fibre bundles of high respiratory capacity, the apparent K_m for ADP increases
725 up to 0.5 mM (Saks *et al.* 1998), consistent with experimental evidence that >90% saturation is reached
726 only at >5 mM ADP (Pesta and Gnaiger 2012). Similar ADP concentrations are also required for
727 accurate determination of OXPHOS-capacity in human clinical cancer samples and permeabilized cells
728 (Klepinin *et al.* 2016; Koit *et al.* 2017). Whereas 2.5 to 5 mM ADP is sufficient to obtain the actual
729 OXPHOS-capacity in many types of permeabilized tissue and cell preparations, experimental validation
730 is required in each specific case.

731 **2.5.3. Electron transfer-state (Figure 6C):** O₂ flux determined in the ET-state yields an estimate
732 of ET-capacity. The ET-state is defined as the *noncoupled* state with kinetically-saturating
733 concentrations of O₂, respiratory substrate and optimum *exogenous* uncoupler concentration for
734 maximum O₂ flux. Uncouplers are weak lipid-soluble acids which function as protonophores. These
735 disrupt the barrier function of the mtIM and thus short circuit the protonmotive system, functioning like
736 a clutch in a mechanical system. As a consequence of the nearly collapsed protonmotive force, the
737 driving force is insufficient for phosphorylation, and $J_{P_s} = 0$. The most frequently used uncouplers are
738 carbonyl cyanide *m*-chloro phenyl hydrazone (CCCP), carbonyl cyanide *p*-
739 trifluoromethoxyphenylhydrazone (FCCP), or dinitrophenole (DNP). Stepwise titration of uncouplers
740 stimulates respiration up to or above the level of O₂ consumption rates in the OXPHOS-state; respiration
741 is inhibited, however, above optimum uncoupler concentrations (Mitchell 2011). Data obtained with a
742 single dose of uncoupler must be evaluated with caution, particularly when a fixed uncoupler
743 concentration is used in studies exploring a treatment or disease that may alter the mitochondrial content
744 or mitochondrial sensitivity to inhibition by uncouplers. The effect on ET-capacity of the reversed
745 function of F-ATPase (J_{P_s} ; **Figure 6C**) can be evaluated in the presence and absence of
746 extramitochondrial ATP.

747 **2.5.4. ROX state and *Rox*:** Besides the three fundamental coupling states of mitochondrial
748 preparations, the state of residual O₂ consumption, ROX, is relevant to assess respiratory function
749 (**Figure 1**). ROX is not a coupling state. The rate of residual oxygen consumption, *Rox*, is defined as O₂
750 consumption due to oxidative reactions measured after inhibition of ET—with rotenone, malonic acid
751 and antimycin A. Cyanide and azide inhibit not only CIV but catalase and several peroxidases involved
752 in *Rox*. High concentrations of antimycin A, but not rotenone or cyanide, inhibit peroxisomal acyl-CoA
753 oxidase and D-amino acid oxidase (Vamecq *et al.* 1987). *Rox* represents a baseline that is used to correct

754 respiration measured in defined coupling states. *Rox*-corrected L , P and E not only lower the values of
 755 total fluxes, but also change the flux control ratios L/P and L/E . *Rox* is not necessarily equivalent to non-
 756 mitochondrial reduction of O_2 , considering O_2 -consuming reactions in mitochondria that are not related
 757 to ET—such as O_2 consumption in reactions catalyzed by monoamine oxidases (type A and B),
 758 monoxygenases (cytochrome P450 monoxygenases), dioxygenase (sulfur dioxygenase and
 759 trimethyllysine dioxygenase), and several hydroxylases. Even isolated mitochondrial fractions,
 760 especially those obtained from liver, may be contaminated by peroxisomes. This fact makes the exact
 761 determination of mitochondrial O_2 consumption and mitochondria-associated generation of reactive
 762 oxygen species complicated (Schönfeld *et al.* 2009; Speijer 2016; **Figure 2**). The dependence of ROX-
 763 linked O_2 consumption needs to be studied in detail together with non-ET enzyme activities, availability
 764 of specific substrates, O_2 concentration, and electron leakage leading to the formation of reactive oxygen
 765 species.

766 **2.5.5. Quantitative relations:** E may exceed or be equal to P . $E > P$ is observed in many types
 767 of mitochondria, varying between species, tissues and cell types (Gnaiger 2009). $E-P$ is the excess ET-
 768 capacity pushing the phosphorylation-flux (**Figure 2C**) to the limit of its *capacity of utilizing* the
 769 protonmotive force. In addition, the magnitude of $E-P$ depends on the tightness of respiratory coupling
 770 or degree of uncoupling, since an increase of L causes P to increase towards the limit of E . The *excess*
 771 $E-P$ capacity, $E-P$, therefore, provides a sensitive diagnostic indicator of specific injuries of the
 772 phosphorylation-pathway, under conditions when E remains constant but P declines relative to controls
 773 (**Figure 5**). Substrate cocktails supporting simultaneous convergent electron transfer to the Q-junction
 774 for reconstitution of TCA cycle function establish pathway control states with high ET-capacity, and
 775 consequently increase the sensitivity of the $E-P$ assay.

776 E cannot theoretically be lower than P . $E < P$ must be discounted as an artefact, which may be
 777 caused experimentally by: (1) loss of oxidative capacity during the time course of the respirometric
 778 assay, since E is measured subsequently to P ; (2) using insufficient uncoupler concentrations; (3) using
 779 high uncoupler concentrations which inhibit ET (Gnaiger 2008); (4) high oligomycin concentrations
 780 applied for measurement of L before titrations of uncoupler, when oligomycin exerts an inhibitory effect
 781 on E . On the other hand, the excess ET-capacity is overestimated if non-saturating [ADP] or $[P_i]$ are
 782 used. See State 3 in the next section.

783 The net OXPHOS-capacity is calculated by subtracting L from P (**Figure 5**). The net $P \gg O_2$ equals
 784 $P \gg (P-L)$, wherein the dissipative LEAK component in the OXPHOS-state may be overestimated. This
 785 can be avoided by measuring LEAK-respiration in a state when the protonmotive force is adjusted to its
 786 slightly lower value in the OXPHOS-state—by titration of an ET inhibitor (Divakaruni and Brand 2011).
 787 Any turnover-dependent components of proton leak and slip, however, are underestimated under these
 788 conditions (Garlid *et al.* 1993). In general, it is inappropriate to use the term *ATP production* or *ATP*
 789 *turnover* for the difference of O_2 flux measured in the OXPHOS and LEAK states. $P-L$ is the upper limit
 790 of OXPHOS-capacity that is freely available for ATP production (corrected for LEAK-respiration) and
 791 is fully coupled to phosphorylation with a maximum mechanistic stoichiometry (**Figure 5**).

792 The rates of LEAK respiration and OXPHOS capacity depend on (1) the tightness of coupling
 793 under the influence of the respiratory uncoupling mechanisms (**Figure 4**), and (2) the coupling
 794 stoichiometry, which varies as a function of the substrate type undergoing oxidation in ET-pathways
 795 with either two or three coupling sites (**Figure 2B**). When cocktails with NADH-linked substrates and
 796 succinate are used, the relative contribution of ET-pathways with three or two coupling sites cannot be
 797 controlled experimentally, is difficult to determine, and may shift in transitions between LEAK-,
 798 OXPHOS- and ET-states (Gnaiger 2014). Under these experimental conditions, we cannot separate the
 799 tightness of coupling *versus* coupling stoichiometry as the mechanisms of respiratory control in the shift
 800 of L/P ratios. The tightness of coupling and fully coupled O_2 flux, $P-L$ (**Table 2**), therefore, are obtained
 801 from measurements of coupling control of LEAK respiration, OXPHOS- and ET-capacities in well
 802 defined pathway states, using either pyruvate and malate as substrates or the classical succinate and
 803 rotenone substrate-inhibitor combination (**Figure 2B**).

804 **2.5.6. The steady-state:** Mitochondria represent a thermodynamically open system in non-
 805 equilibrium states of biochemical energy transformation. State variables (protonmotive force; redox
 806 states) and metabolic *rates* (fluxes) are measured in defined mitochondrial respiratory *states*. Steady-
 807 states can be obtained only in open systems, in which changes by *internal* transformations, *e.g.*, O_2
 808 consumption, are instantaneously compensated for by *external* fluxes, *e.g.*, O_2 supply, preventing a
 809 change of O_2 concentration in the system (Gnaiger 1993b). Mitochondrial respiratory states monitored

810 in closed systems satisfy the criteria of pseudo-steady states for limited periods of time, when changes
 811 in the system (concentrations of O₂, fuel substrates, ADP, P_i, H⁺) do not exert significant effects on
 812 metabolic fluxes (respiration, phosphorylation). Such pseudo-steady states require respiratory media
 813 with sufficient buffering capacity and substrates maintained at kinetically-saturating concentrations, and
 814 thus depend on the kinetics of the processes under investigation.

815

816 2.6. Classical terminology for isolated mitochondria

817 *'When a code is familiar enough, it ceases appearing like a code; one forgets that there is a*
 818 *decoding mechanism. The message is identical with its meaning'* (Hofstadter 1979).

819

820 Chance and Williams (1955; 1956) introduced five classical states of mitochondrial respiration
 821 and cytochrome redox states. **Table 3** shows a protocol with isolated mitochondria in a closed
 822 respirometric chamber, defining a sequence of respiratory states. States and rates are not specifically
 823 distinguished in this nomenclature.

824

825 **Table 3. Metabolic states of mitochondria (Chance and**
 826 **Williams, 1956; Table V).**

827

State	[O ₂]	ADP level	Substrate level	Respiration rate	Rate-limiting substance
1	>0	low	low	slow	ADP
2	>0	high	~0	slow	substrate
3	>0	high	high	fast	respiratory chain
4	>0	low	high	slow	ADP
5	0	high	high	0	oxygen

828

829 **2.6.1. State 1** is obtained after addition of isolated mitochondria to air-saturated
 830 isoosmotic/isotonic respiration medium containing P_i, but no fuel substrates and no adenylates, *i.e.*,
 831 AMP, ADP, ATP.

832 **2.6.2. State 2** is induced by addition of a 'high' concentration of ADP (typically 100 to 300 μM),
 833 which stimulates respiration transiently on the basis of endogenous fuel substrates and phosphorylates
 834 only a small portion of the added ADP. State 2 is then obtained at a low respiratory activity limited by
 835 exhausted endogenous fuel substrate availability (**Table 3**). If addition of specific inhibitors of
 836 respiratory complexes—such as rotenone—does not cause a further decline of O₂ flux, State 2 is
 837 equivalent to the ROX state (See below.). If inhibition is observed, undefined endogenous fuel substrates
 838 are a confounding factor of pathway control, contributing to the effect of subsequently externally added
 839 substrates and inhibitors. In contrast to the original protocol, an alternative sequence of titration steps is
 840 frequently applied, in which the alternative 'State 2' has an entirely different meaning, when this second
 841 state is induced by addition of fuel substrate without ADP or ATP (LEAK-state; in contrast to State 2
 842 defined in **Table 1** as a ROX state). Some researchers have called this condition as "pseudostate 4"
 843 because it has no significant concentrations of adenine nucleotides and hence it is not a near-
 844 physiological condition, although it should be used for calculating the net OXPHOS-capacity, *P-L*.

845 **2.6.3. State 3** is the state stimulated by addition of fuel substrates while the ADP concentration
 846 is still high (**Table 3**) and supports coupled energy transformation through oxidative phosphorylation.
 847 'High ADP' is a concentration of ADP specifically selected to allow the measurement of State 3 to State
 848 4 transitions of isolated mitochondria in a closed respirometric chamber. Repeated ADP titration re-
 849 establishes State 3 at 'high ADP'. Starting at O₂ concentrations near air-saturation (193 or 238 μM O₂
 850 at 37 °C or 25 °C and sea level at 1 atm or 101.32 kPa, and an oxygen solubility of respiration medium
 851 at 0.92 times that of pure water; Forstner and Gnaiger 1983), the total ADP concentration added must
 852 be low enough (typically 100 to 300 μM) to allow phosphorylation to ATP at a coupled O₂ flux that
 853 does not lead to O₂ depletion during the transition to State 4. In contrast, kinetically-saturating ADP
 854 concentrations usually are 10-fold higher than 'high ADP', *e.g.*, 2.5 mM in isolated mitochondria. The
 855 abbreviation State 3u is occasionally used in bioenergetics, to indicate the state of respiration after

856 titration of an uncoupler, without sufficient emphasis on the fundamental difference between OXPHOS-
 857 capacity (*well-coupled* with an *endogenous* uncoupled component) and ET-capacity (*noncoupled*).

858 **2.6.4. State 4** is a LEAK-state that is obtained only if the mitochondrial preparation is intact and
 859 well-coupled. Depletion of ADP by phosphorylation to ATP causes a decline of O₂ flux in the transition
 860 from State 3 to State 4. Under the conditions of State 4, a maximum protonmotive force and high
 861 ATP/ADP ratio are maintained. The gradual decline of $Y_{P\gg/O_2}$ towards diminishing [ADP] at State 4 must
 862 be taken into account for calculation of P_»/O₂ ratios (Gnaiger 2001). State 4 respiration, L_T (**Table 1**),
 863 reflects intrinsic proton leak and ATP hydrolysis activity. O₂ flux in State 4 is an overestimation of
 864 LEAK-respiration if the contaminating ATP hydrolysis activity recycles some ATP to ADP, $J_{P\ll}$, which
 865 stimulates respiration coupled to phosphorylation, $J_{P\gg} > 0$. Some degree of mechanical disruption and
 866 loss of mitochondrial integrity allows the exposed mitochondrial F-ATPases to hydrolyze the ATP
 867 synthesized by the fraction of coupled mitochondria. This can be tested by inhibition of the
 868 phosphorylation-pathway using oligomycin, ensuring that $J_{P\gg} = 0$ (State 4o). On the other hand, the State
 869 4 respiration reached after exhaustion of added ADP is a more physiological condition (*i.e.*, presence of
 870 ATP, ADP and even AMP). Sequential ADP titrations re-establish State 3, followed by State 3 to State
 871 4 transitions while sufficient O₂ is available. Anoxia may be reached, however, before exhaustion of
 872 ADP (State 5).

873 **2.6.5. State 5** is the state after exhaustion of O₂ in a closed respirometric chamber. Diffusion of
 874 O₂ from the surroundings into the aqueous solution may be a confounding factor preventing complete
 875 anoxia (Gnaiger 2001). Chance and Williams (1955) provide an alternative definition of State 5, which
 876 gives it the different meaning of ROX versus anoxia: ‘State 5 may be obtained by antimycin A treatment
 877 or by anaerobiosis’.

878 In **Table 3**, only States 3 and 4 are coupling control states, with the restriction that rates in State
 879 3 may be limited kinetically by non-saturating ADP concentrations.

880

881 2.7. Control and regulation

882

883 The terms metabolic *control* and *regulation* are frequently used synonymously, but are
 884 distinguished in metabolic control analysis: ‘We could understand the regulation as the mechanism that
 885 occurs when a system maintains some variable constant over time, in spite of fluctuations in external
 886 conditions (homeostasis of the internal state). On the other hand, metabolic control is the power to
 887 change the state of the metabolism in response to an external signal’ (Fell 1997). Respiratory control
 888 may be induced by experimental control signals that *exert* an influence on: (1) ATP demand and ADP
 889 phosphorylation-rate; (2) fuel substrate composition, pathway competition; (3) available amounts of
 890 substrates and O₂, *e.g.*, starvation and hypoxia; (4) the protonmotive force, redox states, flux–force
 891 relationships, coupling and efficiency; (5) Ca²⁺ and other ions including H⁺; (6) inhibitors, *e.g.*, nitric
 892 oxide or intermediary metabolites such as oxaloacetate; (7) signalling pathways and regulatory proteins,
 893 *e.g.*, insulin resistance, transcription factor hypoxia inducible factor 1. *Mechanisms* of respiratory
 894 control and regulation include adjustments of: (1) enzyme activities by allosteric mechanisms and
 895 phosphorylation; (2) enzyme content, concentrations of cofactors and conserved moieties—such as
 896 adenylates, nicotinamide adenine dinucleotide [NAD⁺/NADH], coenzyme Q, cytochrome *c*; (3)
 897 metabolic channeling by supercomplexes; and (4) mitochondrial density (enzyme concentrations and
 898 membrane area) and morphology (cristae folding, fission and fusion). Mitochondria are targeted directly
 899 by hormones, *e.g.*, progesterone and glucacorticoids, which affect their energy metabolism (Lee *et al.*
 900 2013; Gerö and Szabo 2016; Price and Dai 2016; Moreno *et al.* 2017). Evolutionary or acquired
 901 differences in the genetic and epigenetic basis of mitochondrial function (or dysfunction) between
 902 individuals; age; biological sex, and hormone concentrations; life style including exercise and nutrition;
 903 and environmental issues including thermal, atmospheric, toxic and pharmacological factors, exert an
 904 influence on all control mechanisms listed above. For reviews, see Brown 1992; Gnaiger 1993a, 2009;
 905 2014; Paradies *et al.* 2014; Morrow *et al.* 2017.

906 Lack of control by a metabolic pathway, *e.g.*, phosphorylation-pathway, means that there will
 907 be no response to a variable activating it, *e.g.*, [ADP]. The reverse, however, is not true as the absence
 908 of a response to [ADP] does not exclude the phosphorylation-pathway from having some degree of
 909 control. The degree of control of a component of the OXPHOS-pathway on an output variable—such
 910 as O₂ flux, will in general be different from the degree of control on other outputs—such as

911 phosphorylation-flux or proton leak flux. Therefore, it is necessary to be specific as to which input and
912 output are under consideration (Fell 1997).

913 Respiratory control refers to the ability of mitochondria to adjust O₂ flux in response to external
914 control signals by engaging various mechanisms of control and regulation. Respiratory control is
915 monitored in a mitochondrial preparation under conditions defined as respiratory states, preferentially
916 under near-physiological conditions of temperature, pH and medium ionic composition, to generate data
917 of higher biological relevance. When phosphorylation of ADP to ATP is stimulated or depressed, an
918 increase or decrease is observed in electron transfer measured as O₂ flux in respiratory coupling states
919 of intact mitochondria ('controlled states' in the classical terminology of bioenergetics). Alternatively,
920 coupling of electron transfer with phosphorylation is diminished by uncouplers. The corresponding
921 coupling control state is characterized by a high respiratory rate without control by P_o (noncoupled or
922 'uncontrolled state').

923
924

925 3. What is a rate?

926

927 The term *rate* is not adequately defined to be useful for reporting data. Normalization of 'rates'
928 leads to a diversity of formats. Application of common and defined units is required for direct transfer
929 of reported results into a database. The second [s] is the SI unit for the base quantity *time*. It is also the
930 standard time-unit used in solution chemical kinetics.

931 The inconsistency of the meanings of rate becomes apparent when considering Galileo Galilei's
932 famous principle, that 'bodies of different weight all fall at the same rate (have a constant acceleration)'
933 (Coopersmith 2010). A rate may be an extensive quantity, which is a *flow*, *I*, when expressed per object
934 (per number of cells or organisms) or per chamber (per system). 'System' is defined as the open or
935 closed chamber of the measuring device. A rate is a *flux*, *J*, when expressed as a size-specific quantity
936 (**Figure 7A; Box 2**).

937 • **Extensive quantities:** An extensive quantity increases proportionally with system size. For
938 example, mass and volume are extensive quantities. Flow is an extensive quantity. The
939 magnitude of an extensive quantity is completely additive for non-interacting subsystems.
940 The magnitude of these quantities depends on the extent or size of the system (Cohen *et al.*
941 2008).

942 • **Size-specific quantities:** 'The adjective *specific* before the name of an extensive quantity is
943 often used to mean *divided by mass*' (Cohen *et al.* 2008). In this system-paradigm, mass-
944 specific flux is flow divided by mass of the *system* (the total mass of everything within the
945 measuring chamber or reactor). Rates are frequently expressed as volume-specific flux. A
946 mass-specific or volume-specific quantity is independent of the extent of non-interacting
947 homogenous subsystems. Tissue-specific quantities (related to the *sample* in contrast to the
948 *system*) are of fundamental interest in the field of comparative mitochondrial physiology,
949 where *specific* refers to the *type of the sample* rather than *mass of the system*. The term
950 *specific*, therefore, must be clarified; *sample-specific*, *e.g.*, muscle mass-specific
951 normalization, is distinguished from *system-specific* quantities (mass or volume; **Figure 7**).

952 • **Intensive quantities:** In contrast to size-specific properties, forces are *intensive* quantities
953 defined as the change of an extensive quantity per advancement of an energy transformation
954 (Gnaiger 1993b).

955 • *N_x* and *m_x* indicate the number format and mass format, respectively, for expressing the
956 quantity of a sample *X*. When different formats are indicated in symbols of derived quantities,
957 the format (*N*, *m*) is shown as a subscript (*underlined italic*), as in *I*_{O₂/*N_x*} and *J*_{O₂/*m_x*}. Oxygen
958 flow and flux are expressed in the molar format, *n*_{O₂} [mol], but in the volume format, *V*_{O₂} [m³]
959 in ergometry. For mass-specific flux these formats can be distinguished as *J*_{*n*O₂/*m_x*} and *J*_{*V*O₂/*m_x*},
960 respectively. Further examples are given in **Figure 7** and **Table 4**.

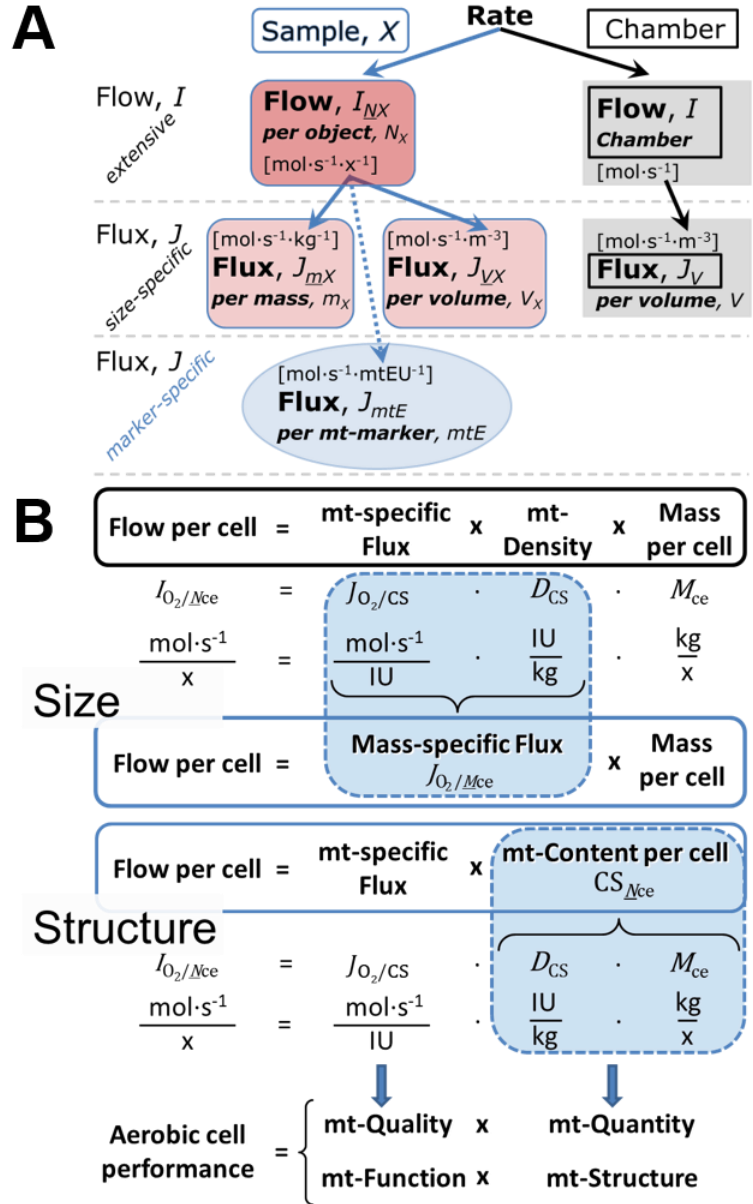
961

962 **Figure 7. Flow and flux, and**
 963 **normalization in structure-**
 964 **function analysis**

965 (A) When expressing metabolic
 966 ‘rate’ measured in a chamber, a
 967 fundamental distinction is made
 968 between relating the rate to the
 969 experimental sample (left) or
 970 chamber (right). The different
 971 meanings of rate need to be
 972 specified by the chosen
 973 normalization. Left: Results are
 974 expressed as mass-specific flux, J_{mX} ,
 975 per mg protein, dry or wet mass. Cell
 976 volume, V_{ce} , may be used for
 977 normalization (volume-specific
 978 flux, J_{Vce}). Right: Flow per chamber,
 979 I , or flux per chamber volume, J_V ,
 980 are merely reported for
 981 methodological reasons.

982 (B) O_2 flow per cell, $I_{O_2/Nce}$, is the
 983 product of mitochondria-specific
 984 flux, mt-density and mass per cell.
 985 Unstructured analysis: performance
 986 is the product of mass-specific flux,
 987 $J_{O_2/MX}$ [$\text{mol}\cdot\text{s}^{-1}\cdot\text{kg}^{-1}$], and size (mass
 988 per cell). Structured analysis:
 989 performance is the product of
 990 mitochondrial function (mt-specific
 991 flux) and structure (mt-content).
 992 Modified from Gnaiger (2014). For
 993 further details see **Table 4**.

994
 995
 996
 997
 998
 999



1000 **Box 2: Metabolic flows and fluxes: vectoral, vectorial, and scalar**
 1001

1002 In a generalization of electrical terms, flow as an extensive quantity (I ; per system) is
 1003 distinguished from flux as a size-specific quantity (J ; per system size). *Flows*, I_{tr} , are defined for all
 1004 transformations as extensive quantities. Electric charge per unit time is electric flow or current, $I_{el} =$
 1005 $dQ_{el}\cdot dt^{-1}$ [$A \equiv C\cdot s^{-1}$]. When dividing I_{el} by size of the system (cross-sectional area of a ‘wire’), we obtain
 1006 flux as a size-specific quantity, which is the current density (surface-density of flow) perpendicular to
 1007 the direction of flux, $J_{el} = I_{el}\cdot A^{-1}$ [$A\cdot m^{-2}$] (Cohen et al. 2008). Fluxes with *spatial* geometric direction and
 1008 magnitude are *vectors*. Vector and scalar *fluxes* are related to flows as $J_{tr} = I_{tr}\cdot A^{-1}$ [$\text{mol}\cdot\text{s}^{-1}\cdot\text{m}^{-2}$] and $J_{tr} =$
 1009 $I_{tr}\cdot V^{-1}$ [$\text{mol}\cdot\text{s}^{-1}\cdot\text{m}^{-3}$], expressing flux as an area-specific vector or volume-specific vectorial or scalar
 1010 quantity, respectively (Gnaiger 1993b). We use the metre–kilogram–second–ampere (MKSA)
 1011 international system of units (*SI*) for general cases ([m], [kg], [s] and [A]), with decimal *SI* prefixes for
 1012 specific applications (**Table 4**).

1013 We suggest to define: (1) *vectoral* fluxes, which are translocations as functions of *gradients* with
 1014 direction in geometric space in continuous systems; (2) *vectorial* fluxes, which describe translocations
 1015 in discontinuous systems and are restricted to information on *compartmental differences* (**Figure 3**,
 1016 transmembrane proton flux); and (3) *scalar* fluxes, which are transformations in a *homogenous* system
 1017 (**Figure 3**, catabolic O_2 flux, J_{KO_2}).

1018 Vectorial transmembrane proton fluxes, J_{mH^+pos} and J_{mH^+neg} , are analyzed in a heterogenous
 1019 compartmental system as a quantity with *directional* but not *spatial* information. Translocation of
 1020 protons across the mtIM has a defined direction, either from the negative compartment (matrix space;
 1021 negative, neg-compartment) to the positive compartment (inter-membrane space; positive, pos-
 1022 compartment) or *vice versa* (**Figure 3**). The arrows defining the direction of the translocation between
 1023 the two vesicular compartments may point upwards or downwards, right or left, without any implication
 1024 that these are actual directions in space. The pos-compartment is neither above nor below the neg-
 1025 compartment in a spatial sense, but can be visualized arbitrarily in a figure in the upper position (**Figure**
 1026 **3**). In general, the *compartmental direction* of vectorial translocation from the neg-compartment to the
 1027 pos-compartment is defined by assigning the initial and final state as *ergodynamic compartments*, H^+_{neg}
 1028 $\rightarrow H^+_{pos}$ or $0 = -1 H^+_{neg} + 1 H^+_{pos}$, related to work (erg = work) that must be performed to lift the proton
 1029 from the lower to the higher electrochemical potential or from the lower to the higher ergodynamic
 1030 compartment (Gnaiger 1993b).

1031 In analogy to *vectorial* translocation, the direction of a *scalar* chemical reaction, $A \rightarrow B$ or $0 = -$
 1032 $1 A + 1 B$, is defined by assigning substrates and products, A and B, as ergodynamic compartments. O_2
 1033 is defined as a substrate in respiratory O_2 consumption (electron acceptor), which together with the fuel
 1034 substrates (electron donors) comprises the substrate compartment of the catabolic reaction. Volume-
 1035 specific scalar O_2 flux is coupled to vectorial translocation, yielding the H^+_{pos}/O_2 ratio (**Figure 2B**).

1036 4. Normalization of rate per sample

1037 The challenges of measuring mitochondrial respiratory flux are matched by those of
 1038 normalization. Normalization (**Table 4**) is guided by physicochemical principles, methodological
 1039 considerations, and conceptual strategies (**Figure 7**).

1040 4.1. Flow: per object

1041 **4.1.1. Number concentration, C_{NX} :** Normalization per sample concentration is routinely required
 1042 to report respiratory data. C_{NX} is the experimental *number concentration* of sample X. In the case of
 1043 animals, e.g., nematodes, $C_{NX} = N_X/V [x \cdot L^{-1}]$, where N_X is the number of organisms in the chamber.
 1044 Similarly, the number of cells per chamber volume is the number concentration of permeabilized or
 1045 intact cells $C_{Nce} = N_{ce}/V [x \cdot L^{-1}]$, where N_{ce} is the number of cells in the chamber (**Table 4**).

1046 **4.1.2. Flow per object, $I_{O_2/NX}$:** O_2 flow per cell is calculated from volume-specific O_2 flux, J_{V,O_2}
 1047 $[nmol \cdot s^{-1} \cdot L^{-1}]$ (per V of the measurement chamber [L]), divided by the number concentration of cells.
 1048 The total cell count is the sum of viable and dead cells, $N_{ce} = N_{vce} + N_{dce}$ (**Table 5**). The cell viability
 1049 index, $VI = N_{vce}/N_{ce}$, is the ratio of viable cells (N_{vce} ; before experimental permeabilization) per total cell
 1050 count. After experimental permeabilization, all cells are permeabilized, $N_{pce} = N_{ce}$. The cell viability
 1051 index can be used to normalize respiration for the number of cells that have been viable before
 1052 experimental permeabilization, $I_{O_2/Nvce} = I_{O_2/Nce}/VI$, considering that mitochondrial respiratory
 1053 dysfunction in dead cells should be eliminated as a confounding factor.

1054 The complexity changes when the object is a whole organism studied as an experimental model.
 1055 The scaling law in respiratory physiology reveals a strong interaction between O_2 flow and individual
 1056 body mass, since *basal* metabolic rate (flow) does not increase linearly with body mass, whereas
 1057 *maximum* mass-specific O_2 flux, \dot{V}_{O_2max} or \dot{V}_{O_2peak} , is approximately constant across a large range of
 1058 individual body mass (Weibel and Hoppeler 2005), with individuals, breeds, and species deviating
 1059 substantially from this relationship. \dot{V}_{O_2peak} of human endurance athletes is 60 to 80 mL $O_2 \cdot min^{-1} \cdot kg^{-1}$
 1060 body mass, converted to $J_{O_2peak/Morg}$ of 45 to 60 nmol $\cdot s^{-1} \cdot g^{-1}$ (Gnaiger 2014; **Table 6**).

1061 4.2. Size-specific flux: per sample size

1062 **4.2.1. Sample concentration, C_{mX} :** Considering permeabilized tissue, homogenate or cells as the
 1063 sample, X, the sample mass is m_X [mg], which is frequently measured as wet or dry weight, W_w or W_d
 1064 [mg], respectively, or as amount of protein, $m_{protein}$. The sample concentration is the mass of the
 1065 subsample per volume of the measurement chamber, $C_{mX} = m_X/V [g \cdot L^{-1} = mg \cdot mL^{-1}]$. X is the type of
 1066 sample—isolated mitochondria, tissue homogenate, permeabilized fibres or cells (**Table 5**).

1073 **Table 4. Sample concentrations and normalization of flux.**
1074

Expression	Symbol	Definition	Unit	Notes
Sample				
identity of sample	X	object: cell, tissue, animal, patient		
number of sample entities X	N_X	number of objects	x	1
mass of sample X	m_X		kg	2
mass of object X	M_X	$M_X = m_X \cdot N_X^{-1}$	$\text{kg} \cdot \text{x}^{-1}$	2
Mitochondria				
mitochondria	mt	$X = \text{mt}$		
amount of mt-elementary components	mtE	quantity of mt-marker	mtEU	
Concentrations				
object number concentration	C_{NX}	$C_{NX} = N_X \cdot V^{-1}$	$\text{x} \cdot \text{m}^{-3}$	3
sample mass concentration	C_{mX}	$C_{mX} = m_X \cdot V^{-1}$	$\text{kg} \cdot \text{m}^{-3}$	
mitochondrial concentration	C_{mtE}	$C_{mtE} = mtE \cdot V^{-1}$	$\text{mtEU} \cdot \text{m}^{-3}$	4
specific mitochondrial density	D_{mtE}	$D_{mtE} = mtE \cdot m_X^{-1}$	$\text{mtEU} \cdot \text{kg}^{-1}$	5
mitochondrial content, mtE per object X	mtE_{NX}	$mtE_{NX} = mtE \cdot N_X^{-1}$	$\text{mtEU} \cdot \text{x}^{-1}$	6
O₂ flow and flux				
flow, system	I_{O_2}	internal flow	$\text{mol} \cdot \text{s}^{-1}$	8
volume-specific flux	J_{V,O_2}	$J_{V,O_2} = I_{O_2} \cdot V^{-1}$	$\text{mol} \cdot \text{s}^{-1} \cdot \text{m}^{-3}$	9
flow per object X	$I_{O_2/NX}$	$I_{O_2/NX} = J_{V,O_2} \cdot C_{NX}^{-1}$	$\text{mol} \cdot \text{s}^{-1} \cdot \text{x}^{-1}$	10
mass-specific flux	$J_{O_2/mX}$	$J_{O_2/mX} = J_{V,O_2} \cdot C_{mX}^{-1}$	$\text{mol} \cdot \text{s}^{-1} \cdot \text{kg}^{-1}$	
mt-marker-specific flux	$J_{O_2/mtE}$	$J_{O_2/mtE} = J_{V,O_2} \cdot C_{mtE}^{-1}$	$\text{mol} \cdot \text{s}^{-1} \cdot \text{mtEU}^{-1}$	11

- 1075 1 The unit x for a number is not used by IUPAC. To avoid confusion, the units [$\text{kg} \cdot \text{x}^{-1}$] and [kg]
1076 distinguish the mass per object from the mass of a sample that may contain any number of objects.
1077 Similarly, the units for flow per system *versus* flow per object are [$\text{mol} \cdot \text{s}^{-1}$] (Note 8) and [$\text{mol} \cdot \text{s}^{-1} \cdot \text{x}^{-1}$]
1078 (Note 10).
- 1079 2 Units are given in the MKSA system (**Box 2**). The *SI* prefix k is used for the *SI* base unit of mass (kg
1080 = 1,000 g). In praxis, various *SI* prefixes are used for convenience, to make numbers easily readable,
1081 e.g., 1 mg tissue, cell or mitochondrial mass instead of 0.000001 kg.
- 1082 3 In case of cells (sample $X = \text{cells}$), the object number concentration is $C_{Nce} = N_{ce} \cdot V^{-1}$, and volume
1083 may be expressed in [$\text{dm}^3 \equiv \text{L}$] or [$\text{cm}^3 = \text{mL}$]. See **Table 5** for different object types.
- 1084 4 mt-concentration is an experimental variable, dependent on sample concentration: (1) $C_{mtE} = mtE \cdot V^{-1}$;
1085 (2) $C_{mtE} = mtE_X \cdot C_{NX}$; (3) $C_{mtE} = C_{mX} \cdot D_{mtE}$.
- 1086 5 If the amount of mitochondria, mtE , is expressed as mitochondrial mass, then D_{mtE} is the mass
1087 fraction of mitochondria in the sample. If mtE is expressed as mitochondrial volume, V_{mt} , and the
1088 mass of sample, m_X , is replaced by volume of sample, V_X , then D_{mtE} is the volume fraction of
1089 mitochondria in the sample.
- 1090 6 $mtE_{NX} = mtE \cdot N_X^{-1} = C_{mtE} \cdot C_{NX}^{-1}$.
- 1091 7 O_2 can be replaced by other chemicals to study different reactions, e.g., ATP, H_2O_2 , or vesicular
1092 compartmental translocations, e.g., Ca^{2+} .
- 1093 8 I_{O_2} and V are defined per instrument chamber as a system of constant volume (and constant
1094 temperature), which may be closed or open. I_{O_2} is abbreviated for I_{rO_2} , i.e., the metabolic or internal
1095 O_2 flow of the chemical reaction r in which O_2 is consumed, hence the negative stoichiometric
1096 number, $\nu_{O_2} = -1$. $I_{rO_2} = d_r n_{O_2} / dt \cdot \nu_{O_2}^{-1}$. If r includes all chemical reactions in which O_2 participates, then
1097 $d_r n_{O_2} = dn_{O_2} - d_e n_{O_2}$, where dn_{O_2} is the change in the amount of O_2 in the instrument chamber and $d_e n_{O_2}$
1098 is the amount of O_2 added externally to the system. At steady state, by definition $dn_{O_2} = 0$, hence $d_r n_{O_2}$
1099 $= -d_e n_{O_2}$.
- 1100 9 J_{V,O_2} is an experimental variable, expressed per volume of the instrument chamber.

- 1101 10 $I_{O_2/NX}$ is a physiological variable, depending on the size of entity X .
 1102 11 There are many ways to normalize for a mitochondrial marker, that are used in different experimental
 1103 approaches: (1) $J_{O_2/mtE} = J_{V,O_2} \cdot C_{mX}^{-1}$; (2) $J_{O_2/mtE} = J_{V,O_2} \cdot C_{mX}^{-1} \cdot D_{mtE}^{-1} = J_{O_2/mX} \cdot D_{mtE}^{-1}$; (3) $J_{O_2/mtE} =$
 1104 $J_{V,O_2} \cdot C_{NX}^{-1} \cdot mtE_{NX}^{-1} = I_{O_2/NX} \cdot mtE_{NX}^{-1}$; (4) $J_{O_2/mtE} = I_{O_2} \cdot mtE^{-1}$. The mt-elementary unit [mtEU] varies depending
 1105 on the mt-marker.
 1106
 1107

Table 5. Sample types, X , abbreviations, and quantification.

Identity of sample	X	N_X	Mass ^a	Volume	mt-Marker
mitochondrial preparation		[x]	[kg]	[m ³]	[mtEU]
isolated mitochondria	imt		m_{mt}	V_{mt}	mtE
tissue homogenate	thom		m_{thom}		mtE_{thom}
permeabilized tissue	pti		m_{pti}		mtE_{pti}
permeabilized fibre	pfi		m_{pfi}		mtE_{pfi}
permeabilized cell	pce	N_{pce}	M_{pce}	V_{pce}	mtE_{pce}
cells ^b	ce	N_{ce}	M_{ce}	V_{ce}	mtE_{ce}
intact cell, viable cell	vce	N_{vce}	M_{vce}	V_{vce}	
dead cell	dce	N_{dce}	M_{dce}	V_{dce}	
organism	org	N_{org}	M_{org}	V_{org}	

^a Instead of mass, the wet weight or dry weight is frequently stated, W_w or W_d . m_X is mass of the sample [kg], M_X is mass of the object [kg·x⁻¹] (Table 4).

^b Total cell count, $N_{ce} = N_{vce} + N_{dce}$

1108
 1109
 1110
 1111
 1112 **4.2.2. Size-specific flux:** Cellular O₂ flow can be compared between cells of identical size. To
 1113 take into account changes and differences in cell size, normalization is required to obtain cell size-
 1114 specific or mitochondrial marker-specific O₂ flux (Renner *et al.* 2003).

- **Mass-specific flux, $J_{O_2/mX}$ [mol·s⁻¹·kg⁻¹]:** Mass-specific flux is obtained by expressing respiration per mass of sample, m_X [mg]. Flow per cell is divided by mass per cell, $J_{O_2/mce} = I_{O_2/Nce}/M_{Nce}$. Or chamber volume-specific flux, J_{V,O_2} , is divided by mass concentration of X in the chamber, $J_{O_2/mX} = J_{V,O_2}/C_{mX}$.

- **Cell volume-specific flux, $J_{O_2/VX}$ [mol·s⁻¹·m⁻³]:** Sample volume-specific flux is obtained by expressing respiration per volume of sample. For example, in the case of using cells as sample will be the volume of cells added to the chamber (Figure 7).

1119 If size-specific O₂ flux is constant and independent of sample size, then there is no interaction
 1120 between the subsystems. For example, a 1.5 mg and a 3.0 mg muscle sample respire at identical mass-
 1121 specific flux. Mass-specific O₂ flux, however, may change with the mass of a tissue sample, cells or
 1122 isolated mitochondria in the measuring chamber, in which the nature of the interaction becomes an issue.
 1123 Therefore, cell density must be optimized, particularly in experiments carried out in wells, considering
 1124 the confluency of the cell monolayer or clumps of cells (Salabei *et al.* 2014).
 1125
 1126
 1127
 1128

1129 4.3. Marker-specific flux: per mitochondrial content

1130
 1131 Tissues can contain multiple cell populations that may have distinct mitochondrial subtypes.
 1132 Mitochondria undergo dynamic fission and fusion cycles, and can exist in multiple stages and sizes that
 1133 may be altered by a range of factors. The isolation of mitochondria (often achieved through differential
 1134 centrifugation) can therefore yield a subsample of the mitochondrial types present in a tissue, depending
 1135 on the isolation protocols utilized (*e.g.*, centrifugation speed). This possible bias should be taken into
 1136 account when planning experiments using isolated mitochondria. Different sizes of mitochondria are
 1137 enriched at specific centrifugation speeds, which can be used strategically for isolation of mitochondrial
 1138 subpopulations.

1139 Part of the mitochondrial content of a tissue is lost during preparation of isolated mitochondria.
 1140 The fraction of isolated mitochondria obtained from a tissue sample is expressed as mitochondrial
 1141 recovery. At a high mitochondrial recovery the fraction of isolated mitochondria is more representative
 1142 of the total mitochondrial population than in preparations characterized by low recovery. Determination
 1143 of the mitochondrial recovery and yield is based on measurement of the concentration of a mitochondrial

1144 marker in the stock of isolated mitochondria, $C_{mtE,stock}$, and crude tissue homogenate, $C_{mtE,thom}$, which
 1145 simultaneously provides information on the specific mitochondrial density in the sample, D_{mtE} (Table
 1146 4).

1147 When discussing concepts on normalization, it is essential to consider the question of the study.
 1148 If the study aims at comparing tissue performance—such as the effects of a treatment on a specific
 1149 tissue, then normalization for tissue mass or protein content is appropriate. However, if the aim is to
 1150 find differences on mitochondrial function independent of mitochondrial density (Table 4), then
 1151 normalization to a mitochondrial marker is imperative (Figure 7). One cannot assume that quantitative
 1152 changes in various markers—such as mitochondrial proteins—necessarily occur in parallel with one
 1153 another. It should be established that the marker chosen is not selectively altered by the performed
 1154 treatment. In conclusion, the normalization must reflect the question under investigation to reach a
 1155 satisfying answer. On the other hand, the goal of comparing results across projects and institutions
 1156 requires standardization on normalization for entry into a databank.

1157 **4.3.1. Mitochondrial concentration, C_{mtE} , and mitochondrial markers:** Mitochondrial
 1158 organelles comprise a dynamic cellular reticulum in various states of fusion and fission. Hence, the
 1159 definition of an "amount" of mitochondria is often misconceived: mitochondria cannot be counted
 1160 reliably as a number of occurring elementary components. Therefore, quantification of the "amount" of
 1161 mitochondria depends on the measurement of chosen mitochondrial markers. 'Mitochondria are the
 1162 structural and functional elementary units of cell respiration' (Gnaiger 2014). The quantity of a
 1163 mitochondrial marker can reflect the amount of *mitochondrial elementary components*, mtE , expressed
 1164 in various mitochondrial elementary units [mtEU] specific for each measured mt-marker (Table 4).
 1165 However, since mitochondrial quality may change in response to stimuli—particularly in mitochondrial
 1166 dysfunction (Campos *et al.* 2017) and after exercise training (Pesta *et al.* 2011) and during aging (Daum
 1167 *et al.* 2013)—some markers can vary while others are unchanged: (1) Mitochondrial volume and
 1168 membrane area are structural markers, whereas mitochondrial protein mass is commonly used as a
 1169 marker for isolated mitochondria. (2) Molecular and enzymatic mitochondrial markers (amounts or
 1170 activities) can be selected as matrix markers, *e.g.*, citrate synthase activity, mtDNA; mtIM-markers, *e.g.*,
 1171 cytochrome *c* oxidase activity, aa_3 content, cardiolipin, or mtOM-markers, *e.g.*, the voltage-dependent
 1172 anion channel (VDAC), TOM20. (3) Extending the measurement of mitochondrial marker enzyme
 1173 activity to mitochondrial pathway capacity, ET- or OXPHOS-capacity can be considered as an
 1174 integrative functional mitochondrial marker.

1175 Depending on the type of mitochondrial marker, the mitochondrial elementary component, mtE ,
 1176 is expressed in marker-specific units. Mitochondrial concentration in the measurement chamber and the
 1177 tissue of origin are quantified as (1) a quantity for normalization in functional analyses, C_{mtE} , and (2) a
 1178 physiological output that is the result of mitochondrial biogenesis and degradation, D_{mtE} , respectively
 1179 (Table 4). It is recommended, therefore, to distinguish *experimental mitochondrial concentration*, C_{mtE}
 1180 $= mtE/V$ and *physiological mitochondrial density*, $D_{mtE} = mtE/m_X$. Then mitochondrial density is the
 1181 amount of mitochondrial elementary components per mass of tissue, which is a biological variable
 1182 (Figure 7). The experimental variable is mitochondrial density multiplied by sample mass concentration
 1183 in the measuring chamber, $C_{mtE} = D_{mtE} \cdot C_{m_X}$, or mitochondrial content multiplied by sample number
 1184 concentration, $C_{mtE} = mtE_X \cdot C_{N_X}$ (Table 4).

1185 **4.3.2. mt-Marker-specific flux, $J_{O_2/mtE}$:** Volume-specific metabolic O_2 flux depends on: (1) the
 1186 sample concentration in the volume of the instrument chamber, C_{m_X} , or C_{N_X} ; (2) the mitochondrial
 1187 density in the sample, $D_{mtE} = mtE/m_X$ or $mtE_X = mtE/N_X$; and (3) the specific mitochondrial activity or
 1188 performance per elementary mitochondrial unit, $J_{O_2/mtE} = J_{V,O_2}/C_{mtE}$ [$mol \cdot s^{-1} \cdot mtEU^{-1}$] (Table 4).
 1189 Obviously, the numerical results for $J_{O_2/mtE}$ vary with the type of mitochondrial marker chosen for
 1190 measurement of mtE and $C_{mtE} = mtE/V$ [$mtEU \cdot m^{-3}$].

1191 Different methods are implicated in the quantification of mitochondrial markers and have
 1192 different strengths. Some problems are common for all mitochondrial markers, mtE : (1) Accuracy of
 1193 measurement is crucial, since even a highly accurate and reproducible measurement of O_2 flux results
 1194 in an inaccurate and noisy expression if normalized by a biased and noisy measurement of a
 1195 mitochondrial marker. This problem is acute in mitochondrial respiration because the denominators used
 1196 (the mitochondrial markers) are often small moieties of which accurate and precise determination is
 1197 difficult. This problem can be avoided when O_2 fluxes measured in substrate-uncoupler-inhibitor
 1198 titration protocols are normalized for flux in a defined respiratory reference state, which is used as an
 1199 *internal* marker and yields flux control ratios, $FCRs$. $FCRs$ are independent of *externally* measured

1200 markers and, therefore, are statistically robust, considering the limitations of ratios in general (Jasienski
 1201 and Bazzaz 1999). *FCRs* indicate qualitative changes of mitochondrial respiratory control, with highest
 1202 quantitative resolution, separating the effect of mitochondrial density or concentration on $J_{O_2/mX}$ and
 1203 $I_{O_2/mX}$ from that of function per elementary mitochondrial marker, $J_{O_2/mtE}$ (Pesta *et al.* 2011; Gnaiger
 1204 2014). (2) If mitochondrial quality does not change and only the amount of mitochondria varies as a
 1205 determinant of mass-specific flux, any marker is equally qualified in principle; then in practice selection
 1206 of the optimum marker depends only on the accuracy and precision of measurement of the mitochondrial
 1207 marker. (3) If mitochondrial flux control ratios change, then there may not be any best mitochondrial
 1208 marker. In general, measurement of multiple mitochondrial markers enables a comparison and
 1209 evaluation of normalization for a variety of mitochondrial markers. Particularly during postnatal
 1210 development, the activity of marker enzymes—such as cytochrome *c* oxidase and citrate synthase—
 1211 follows different time courses (Drahota *et al.* 2004). Evaluation of mitochondrial markers in healthy
 1212 controls is insufficient for providing guidelines for application in the diagnosis of pathological states
 1213 and specific treatments.

1214 In line with the concept of the respiratory control ratio (Chance and Williams 1955a), the most
 1215 readily used normalization is that of flux control ratios and flux control factors (Gnaiger 2014). Selection
 1216 of the state of maximum flux in a protocol as the reference state has the advantages of: (1) internal
 1217 normalization; (2) statistically validated linearization of the response in the range of 0 to 1; and (3)
 1218 consideration of maximum flux for integrating a large number of elementary steps in the OXPHOS- or
 1219 ET-pathways. This reduces the risk of selecting a functional marker that is specifically altered by the
 1220 treatment or pathology, yet increases the chance that the highly integrative pathway is disproportionately
 1221 affected, *e.g.*, the OXPHOS- rather than ET-pathway in case of an enzymatic defect in the
 1222 phosphorylation-pathway. In this case, additional information can be obtained by reporting flux control
 1223 ratios based on a reference state which indicates stable tissue-mass specific flux.

1224 Stereological determination of mitochondrial content via two-dimensional transmission electron
 1225 microscopy can have limitations due to the dynamics of mitochondrial size (Meinild Lundby *et al.*
 1226 2017). Accurate determination of three-dimensional volume by two-dimensional microscopy can be
 1227 both time consuming and statistically challenging (Larsen *et al.* 2012).

1228 The validity of using mitochondrial marker enzymes (citrate synthase activity, CI to CIV amount
 1229 or activity) for normalization of flux is limited in part by the same factors that apply to flux control
 1230 ratios. Strong correlations between various mitochondrial markers and citrate synthase activity
 1231 (Reichmann *et al.* 1985; Boushel *et al.* 2007; Mogensen *et al.* 2007) are expected in a specific tissue of
 1232 healthy persons and in disease states not specifically targeting citrate synthase. Citrate synthase activity
 1233 is acutely modifiable by exercise (Tonkonogi *et al.* 1997; Leek *et al.* 2001). Evaluation of mitochondrial
 1234 markers related to a selected age and sex cohort cannot be extrapolated to provide recommendations for
 1235 normalization in respirometric diagnosis of disease, in different states of development and ageing,
 1236 different cell types, tissues, and species. mtDNA normalized to nDNA via qPCR is correlated to
 1237 functional mitochondrial markers including OXPHOS- and ET-capacity in some cases (Puntschart *et al.*
 1238 1995; Wang *et al.* 1999; Menshikova *et al.* 2006; Boushel *et al.* 2007; Ehinger *et al.* 2015), but lack of
 1239 such correlations have been reported (Menshikova *et al.* 2005; Schultz and Wiesner 2000; Pesta *et al.*
 1240 2011). Several studies indicate a strong correlation between cardiolipin content and increase in
 1241 mitochondrial function with exercise (Menshikova *et al.* 2005; Menshikova *et al.* 2007; Larsen *et al.*
 1242 2012; Faber *et al.* 2014), but it has not been evaluated as a general mitochondrial biomarker in disease.
 1243 With no single best mitochondrial marker, a good strategy is to quantify several different biomarkers to
 1244 minimize the decorrelating effects caused by diseases, treatments, or other factors. Determination of
 1245 multiple markers, particularly a matrix marker and a marker from the mtIM, allows tracking changes in
 1246 mitochondrial quality defined by their ratio.

1247 5. Normalization of rate per system

1248 5.1. Flow: per chamber

1249 The experimental system (experimental chamber) is part of the measurement instrument,
 1250 separated from the environment as an isolated, closed, open, isothermal or non-isothermal system
 1251 (Table 4). Reporting O_2 flows per respiratory chamber, I_{O_2} [$\text{nmol}\cdot\text{s}^{-1}$], restricts the analysis to intra-
 1252 experimental comparison of relative differences.

5.2. Flux: per chamber volume

5.2.1. System-specific flux, J_{V,O_2} : We distinguish between (1) the *system* with volume V and mass m defined by the system boundaries, and (2) the *sample* or *objects* with volume V_X and mass m_X that are enclosed in the experimental chamber (**Figure 7**). Metabolic O_2 flow per object, $I_{O_2/NX}$, is the total O_2 flow in the system divided by the number of objects, N_X , in the system. $I_{O_2/NX}$ increases as the mass of the object is increased. Sample mass-specific O_2 flux, $J_{O_2/mX}$ should be independent of the mass of the sample studied in the instrument chamber, but system volume-specific O_2 flux, J_{V,O_2} (per volume of the instrument chamber), increases in proportion to the mass of the sample in the chamber. Whereas J_{V,O_2} depends on mass-concentration of the sample in the chamber, it should be independent of the chamber (system) volume at constant sample mass. There are practical limitations to increase the mass-concentration of the sample in the chamber, when one is concerned about crowding effects and instrumental time resolution.

5.2.2. Advancement per volume: When the reactor volume does not change during the reaction, which is typical for liquid phase reactions, the volume-specific flux of a chemical reaction r is the time derivative of the advancement of the reaction per unit volume, $J_{V,rB} = d_t \xi_B / dt \cdot V^{-1}$ [(mol·s⁻¹)·L⁻¹]. The rate of concentration change is dc_B/dt [(mol·L⁻¹)·s⁻¹], where concentration is $c_B = n_B/V$. There is a difference between (1) J_{V,rO_2} [mol·s⁻¹·L⁻¹] and (2) rate of concentration change [mol·L⁻¹·s⁻¹]. These merge to a single expression only in closed systems. In open systems, internal transformations (catabolic flux, O_2 consumption) are distinguished from external flux (such as O_2 supply). External fluxes of all substances are zero in closed systems. In a closed chamber O_2 consumption (internal flux of catabolic reactions k), I_{kO_2} [pmol·s⁻¹], causes a decline of the amount of O_2 in the system, n_{O_2} [nmol]. Normalization of these quantities for the volume of the system, V [L \equiv dm³], yields volume-specific O_2 flux, $J_{V,kO_2} = I_{kO_2}/V$ [nmol·s⁻¹·L⁻¹], and O_2 concentration, $[O_2]$ or $c_{O_2} = n_{O_2}/V$ [μ mol·L⁻¹ = μ M = nmol·mL⁻¹]. Instrumental background O_2 flux is due to external flux into a non-ideal closed respirometer; then total volume-specific flux has to be corrected for instrumental background O_2 flux— O_2 diffusion into or out of the instrumental chamber. J_{V,kO_2} is relevant mainly for methodological reasons and should be compared with the accuracy of instrumental resolution of background-corrected flux, e.g., ± 1 nmol·s⁻¹·L⁻¹ (Gnaiger 2001). ‘Metabolic’ or catabolic indicates O_2 flux, J_{kO_2} , corrected for: (1) instrumental background O_2 flux; (2) chemical background O_2 flux due to autoxidation of chemical components added to the incubation medium; and (3) *Rox* for O_2 -consuming side reactions unrelated to the catabolic pathway k .

6. Conversion of units

Many different units have been used to report the O_2 consumption rate, OCR (**Table 6**). SI base units provide the common reference to introduce the theoretical principles (**Figure 7**), and are used with appropriately chosen *SI* prefixes to express numerical data in the most practical format, with an effort towards unification within specific areas of application (**Table 7**). Reporting data in *SI* units—including the mole [mol], coulomb [C], joule [J], and second [s]—should be encouraged, particularly by journals which propose the use of *SI* units.

Although volume is expressed as m³ using the *SI* base unit, the litre [dm³] is a conventional unit of volume for concentration and is used for most solution chemical kinetics. If one multiplies $I_{O_2/Nce}$ by C_{Nce} , then the result will not only be the amount of O_2 [mol] consumed per time [s⁻¹] in one litre [L⁻¹], but also the change in O_2 concentration per second (for any volume of an ideally closed system). This is ideal for kinetic modeling as it blends with chemical rate equations where concentrations are typically expressed in mol·L⁻¹ (Wagner *et al.* 2011). In studies of multinuclear cells—such as differentiated skeletal muscle cells—it is easy to determine the number of nuclei but not the total number of cells. A generalized concept, therefore, is obtained by substituting cells by nuclei as the sample entity. This does not hold, however, for enucleated platelets.

For studies of cells, we recommend that respiration be expressed, as far as possible, as: (1) O_2 flux normalized for a mitochondrial marker, for separation of the effects of mitochondrial quality and content on cell respiration (this includes *FCRs* as a normalization for a functional mitochondrial marker); (2) O_2 flux in units of cell volume or mass, for comparison of respiration of cells with different cell size (Renner *et al.* 2003) and with studies on tissue preparations, and (3) O_2 flow in units of attomole (10^{-18} mol) of O_2 consumed in a second by each cell [amol·s⁻¹·cell⁻¹], numerically equivalent to [pmol·s⁻¹· 10^{-6} cells]. This convention allows information to be easily used when designing experiments

1312 in which O₂ flow must be considered. For example, to estimate the volume-specific O₂ flux in an
 1313 instrument chamber that would be expected at a particular cell number concentration, one simply needs
 1314 to multiply the flow per cell by the number of cells per volume of interest. This provides the amount of
 1315 O₂ [mol] consumed per time [s⁻¹] per unit volume [L⁻¹]. At an O₂ flow of 100 amol·s⁻¹·cell⁻¹ and a cell
 1316 density of 10⁹ cells·L⁻¹ (10⁶ cells·mL⁻¹), the volume-specific O₂ flux is 100 nmol·s⁻¹·L⁻¹ (100
 1317 pmol·s⁻¹·mL⁻¹).

1318

1319 **Table 6. Conversion of various formats and units used in respirometry and**
 1320 **ergometry.** e⁻ is the number of electrons or reducing equivalents. z_B is the charge number
 1321 of entity B.
 1322

Format	1 Unit		Multiplication factor	SI-unit	Notes
\underline{n}	ng.atom O·s ⁻¹	(2 e ⁻)	0.5	nmol O ₂ ·s ⁻¹	
\underline{n}	ng.atom O·min ⁻¹	(2 e ⁻)	8.33	pmol O ₂ ·s ⁻¹	
\underline{n}	natom O·min ⁻¹	(2 e ⁻)	8.33	pmol O ₂ ·s ⁻¹	
\underline{n}	nmol O ₂ ·min ⁻¹	(4 e ⁻)	16.67	pmol O ₂ ·s ⁻¹	
\underline{n}	nmol O ₂ ·h ⁻¹	(4 e ⁻)	0.2778	pmol O ₂ ·s ⁻¹	
\underline{V} to \underline{n}	mL O ₂ ·min ⁻¹ at STPD ^a		0.744	μmol O ₂ ·s ⁻¹	1
\underline{e} to \underline{n}	W = J/s at -470 kJ/mol O ₂		-2.128	μmol O ₂ ·s ⁻¹	
\underline{e} to \underline{n}	mA = mC·s ⁻¹	(z _{H+} = 1)	10.36	nmol H ⁺ ·s ⁻¹	2
\underline{e} to \underline{n}	mA = mC·s ⁻¹	(z _{O2} = 4)	2.59	nmol O ₂ ·s ⁻¹	2
\underline{n} to \underline{e}	nmol H ⁺ ·s ⁻¹	(z _{H+} = 1)	0.09649	mA	3
\underline{n} to \underline{e}	nmol O ₂ ·s ⁻¹	(z _{O2} = 4)	0.38594	mA	3

1323 1 At standard temperature and pressure dry (STPD: 0 °C = 273.15 K and 1 atm = 101.325 kPa =
 1324 760 mmHg), the molar volume of an ideal gas, V_m, and V_{m,O₂} is 22.414 and 22.392 L·mol⁻¹,
 1325 respectively. Rounded to three decimal places, both values yield the conversion factor of 0.744.
 1326 For comparison at normal temperature and pressure dry (NTPD: 20 °C), V_{m,O₂} is 24.038 L·mol⁻¹.
 1327 Note that the SI standard pressure is 100 kPa.

1328 2 The multiplication factor is 10⁶/(z_B·F).

1329 3 The multiplication factor is z_B·F/10⁶.

1330

1331 ET-capacity in human cell types including HEK 293, primary HUVEC and fibroblasts ranges
 1332 from 50 to 180 amol·s⁻¹·cell⁻¹, measured in intact cells in the noncoupled state (see Gnaiger 2014). At
 1333 100 amol·s⁻¹·cell⁻¹ corrected for *Rox*, the current across the mt-membranes, I_{H+e}, approximates 193
 1334 pA·cell⁻¹ or 0.2 nA per cell. See Rich (2003) for an extension of quantitative bioenergetics from the
 1335 molecular to the human scale, with a transmembrane proton flux equivalent to 520 A in an adult at a
 1336 catabolic power of -110 W. Modelling approaches illustrate the link between protonmotive force and
 1337 currents (Willis *et al.* 2016).

1338 We consider isolated mitochondria as powerhouses and proton pumps as molecular machines to
 1339 relate experimental results to energy metabolism of the intact cell. The cellular P»/O₂ based on oxidation
 1340 of glycogen is increased by the glycolytic (fermentative) substrate-level phosphorylation of 3 P»/Glyc
 1341 or 0.5 mol P» for each mol O₂ consumed in the complete oxidation of a mol glycosyl unit (Glyc). Adding
 1342 0.5 to the mitochondrial P»/O₂ ratio of 5.4 yields a bioenergetic cell physiological P»/O₂ ratio close to
 1343 6. Two NADH equivalents are formed during glycolysis and transported from the cytosol into the
 1344 mitochondrial matrix, either by the malate-aspartate shuttle or by the glycerophosphate shuttle (**Figure**
 1345 **2A**) resulting in different theoretical yields of ATP generated by mitochondria, the energetic cost of
 1346 which potentially must be taken into account. Considering also substrate-level phosphorylation in the
 1347 TCA cycle, this high P»/O₂ ratio not only reflects proton translocation and OXPHOS studied in isolation,
 1348 but integrates mitochondrial physiology with energy transformation in the living cell (Gnaiger 1993a).

1349

1350

1351 **Table 7. Conversion of units with preservation of numerical values.**

Name	Frequently used unit	Equivalent unit	Notes
volume-specific flux, J_{V,O_2}	$\text{pmol}\cdot\text{s}^{-1}\cdot\text{mL}^{-1}$	$\text{nmol}\cdot\text{s}^{-1}\cdot\text{L}^{-1}$	1
cell-specific flow, $I_{O_2/\text{cell}}$	$\text{mmol}\cdot\text{s}^{-1}\cdot\text{L}^{-1}$	$\text{mol}\cdot\text{s}^{-1}\cdot\text{m}^{-3}$	
	$\text{pmol}\cdot\text{s}^{-1}\cdot 10^{-6}$ cells	$\text{amol}\cdot\text{s}^{-1}\cdot\text{cell}^{-1}$	2
cell number concentration, C_{Nce}	$\text{pmol}\cdot\text{s}^{-1}\cdot 10^{-9}$ cells	$\text{zmol}\cdot\text{s}^{-1}\cdot\text{cell}^{-1}$	3
	10^6 cells $\cdot\text{mL}^{-1}$	10^9 cells $\cdot\text{L}^{-1}$	
mitochondrial protein concentration, C_{mtE}	0.1 mg $\cdot\text{mL}^{-1}$	0.1 g $\cdot\text{L}^{-1}$	
mass-specific flux, $J_{O_2/m}$	$\text{pmol}\cdot\text{s}^{-1}\cdot\text{mg}^{-1}$	$\text{nmol}\cdot\text{s}^{-1}\cdot\text{g}^{-1}$	4
catabolic power, P_k	$\mu\text{W}\cdot 10^{-6}$ cells	$\text{pW}\cdot\text{cell}^{-1}$	1
volume	1,000 L	m^3 (1,000 kg)	
	L	dm^3 (kg)	
	mL	cm^3 (g)	
	μL	mm^3 (mg)	
	fL	μm^3 (pg)	5
amount of substance concentration	$\text{M} = \text{mol}\cdot\text{L}^{-1}$	$\text{mol}\cdot\text{dm}^{-3}$	

1352 1 pmol: picomole = 10^{-12} mol1353 2 amol: attomole = 10^{-18} mol1354 3 zmol: zeptomole = 10^{-21} mol

1355

1356

7. Conclusions

1357

1358 Catabolic cell respiration is the process of exergonic and exothermic energy transformation in

1359 which scalar redox reactions are coupled to vectorial ion translocation across a semipermeable

1360 membrane, which separates the small volume of a bacterial cell or mitochondrion from the larger volume

1361 of its surroundings. The electrochemical exergy can be partially conserved in the phosphorylation of

1362 ADP to ATP or in ion pumping, or dissipated in an electrochemical short-circuit. Respiration is thus

1363 clearly distinguished from fermentation as the counterpart of cellular core energy metabolism. An O_2 1364 flux balance scheme illustrates the relationships and general definitions (**Figures 1 and 2**).

1365

1366

Box 3: Recommendations for studies with mitochondrial preparations

1367

- Normalization of respiratory rates should be provided as far as possible:

1368 1. *Biophysical normalization*: on a per cell basis as O_2 flow; this may not be possible when

1369 dealing with coenocytic organisms or tissues without cross-walls separating individual

1370 cells (e.g., filamentous fungi, muscle fibers)

1371 2. *Cellular normalization*: per g protein; per cell- or tissue-mass as mass-specific O_2 flux;

1372 per cell volume as cell volume-specific flux

1373 3. *Mitochondrial normalization*: per mitochondrial marker as mt-specific flux.

1374 With information on cell size and the use of multiple normalizations, maximum potential information

1375 is available (Renner *et al.* 2003; Wagner *et al.* 2011; Gnaiger 2014). Reporting flow in a respiratory1376 chamber [$\text{nmol}\cdot\text{s}^{-1}$] is discouraged, since it restricts the analysis to intra-experimental comparison of

1377 relative (qualitative) differences.

1378

1379 • Catabolic mitochondrial respiration is distinguished from residual O_2 consumption. Fluxes in1380 mitochondrial coupling states should be, as far as possible, corrected for residual O_2 consumption.

1381 • Different mechanisms of uncoupling should be distinguished by defined terms. The tightness of

1382 coupling relates to these uncoupling mechanisms, whereas the coupling stoichiometry varies as a

1383 function the substrate type involved in ET-pathways with either three or two redox proton pumps

1384 operating in series. Separation of tightness of coupling from the pathway-dependent coupling

1385 stoichiometry is possible only when the substrate type undergoing oxidation remains the same for

1386 respiration in LEAK-, OXPHOS-, and ET-states. In studies of the tightness of coupling, therefore,

- 1387 simple substrate-inhibitor combinations should be applied to exclude a shift in substrate competition
 1388 which may occur when providing physiological substrate cocktails.
- 1389 ● In studies of isolated mitochondria, the mitochondrial recovery and yield should be reported.
 1390 Experimental criteria for evaluation of purity versus integrity should be considered. Mitochondrial
 1391 markers—such as citrate synthase activity as an enzymatic matrix marker—provide a link to the
 1392 tissue of origin on the basis of calculating the mitochondrial recovery, *i.e.*, the fraction of
 1393 mitochondrial marker obtained from a unit mass of tissue. Total mitochondrial protein is frequently
 1394 applied as a mitochondrial marker, which is restricted to isolated mitochondria.
 - 1395 ● In studies of permeabilized cells, the viability of the cell culture or cell suspension of origin should
 1396 be reported. Normalization should be evaluated for total cell count or viable cell count.
 - 1397 ● Terms and symbols are summarized in **Table 8**. Their use will facilitate transdisciplinary
 1398 communication and support further developments towards a consistent theory of bioenergetics and
 1399 mitochondrial physiology. Technical terms related to and defined with normal words can be used as
 1400 index terms in databases, support the creation of ontologies towards semantic information processing
 1401 (MitoPedia), and help in communicating analytical findings as impactful data-driven stories.
 1402 ‘*Making data available without making it understandable may be worse than not making it available*
 1403 *at all*’ (National Academies of Sciences, Engineering, and Medicine 2018). Success will depend on
 1404 taking next steps: (1) exhaustive text-mining considering Omics data and functional data; (2) network
 1405 analysis of Omics data with bioinformatics tools; (3) cross-validation with distinct bioinformatics
 1406 approaches; (4) correlation with functional data; (5) guidelines for biological validation of network
 1407 data. This is a call to carefully contribute to FAIR principles (Findable, Accessible, Interoperable,
 1408 Reusable) for the sharing of scientific data.

1410
 1411 **Table 8. Terms, symbols, and units.**
 1412

1413 Term	1414 Symbol	1415 Unit	1416 Links and comments
1417 alternative quinol oxidase	1418 AOX		1419 Figure 2B
1420 amount of substance B	1421 n_B	1422 [mol]	
1423 ATP yield per O ₂	1424 $Y_{P \gg O_2}$		1425 P \gg /O ₂ ratio measured in any 1426 respiratory state
1427 catabolic reaction	1428 k		1429 Figure 1 and 3
1430 catabolic respiration	1431 J_{kO_2}	1432 <i>varies</i>	1433 Figure 1 and 3
1434 cell number	1435 N_{ce}	1436 [x]	1437 $N_{ce} = N_{vce} + N_{dce}$; Table 5
1438 cell respiration	1439 J_{rO_2}	1440 <i>varies</i>	1441 Figure 1
1442 cell viability index	1443 VI		1444 $VI = N_{vce}/N_{ce} = 1 - N_{dce}/N_{ce}$
1445 Complexes I to IV	1446 CI to CIV		1447 respiratory ET Complexes; Figure 1448 2B
1449 concentration of substance B	1450 $c_B = n_B \cdot V^{-1}$; [B]	1451 [mol·m ⁻³]	1452 Box 2
1453 coupling control state	1454 CCS		1455 ##
1456 dead cell number	1457 N_{dce}	1458 [x]	1459 non-viable cells, loss of plasma 1460 membrane barrier function; Table 5
1461 electric format	1462 e	1463 [C]	1464 Table 6
1465 electron transfer system	1466 ETS		1467 state; Figure 2B, Figure 5
1468 flow, for substance B	1469 I_B	1470 [mol·s ⁻¹]	1471 system-related extensive quantity; 1472 Figure 7
1473 flux, for substance B	1474 J_B	1475 <i>varies</i>	1476 size-specific quantity; Figure 7
1477 inorganic phosphate	1478 P _i		1479 Figure 3
1480 intact cell number, 1481 viable cell number	1482 N_{vce}	1483 [x]	1484 viable cells, intact of plasma 1485 membrane barrier function; Table 5
1486 LEAK state	1487 LEAK		1488 state; Table 1, Figure 5

1442	mass format	\underline{m}	[kg]	Table 4, Figure 7
1443	mass of sample X	m_X	[kg]	Table 4
1444	mass, dry mass	m_d	[kg]	mass of sample X ; Figure 7
1445				(frequently called dry weight)
1446	mass, wet mass	m_w	[kg]	mass of sample X ; Figure 7
1447				(frequently called wet weight)
1448	mass of object X	$M_X = m_X N_X^{-1}$	[kg·x ⁻¹]	mass of entity X ; Table 4
1449	MITOCARTA			https://www.broadinstitute.org/scientific-community/science/programs/metabolic-disease-program/publications/mitocarta/mitocarta-in-0
1450				
1451				
1452				
1453				
1454	MitoPedia			http://www.bioblast.at/index.php/MitoPedia
1455	mitochondria or mitochondrial	mt		Box 1
1456	mitochondrial DNA	mtDNA		Box 1
1457	mitochondrial concentration	$C_{mtE} = mtE \cdot V^{-1}$	[mtEU·m ⁻³]	Table 4
1458	mitochondrial content	mtE_X	[mtEU·x ⁻¹]	$mtE_X = mtE \cdot N_X^{-1}$; Table 4
1459	mitochondrial			
1460	elementary component	mtE	[mtEU]	quantity of mt-marker; Table 4
1461	mitochondrial elementary unit	mtEU	<i>varies</i>	specific units for mt-marker; Table 4
1462	mitochondrial inner membrane	mtIM		MIM is widely used; the first M is replaced by mt; Figure 2; Box 1
1463				MOM is widely used; the first M is replaced by mt; Figure 2; Box 1
1464	mitochondrial outer membrane	mtOM		
1465				
1466	mitochondrial recovery	Y_{mtE}		fraction of mtE recovered in sample from the tissue of origin
1467				
1468	mitochondrial yield	$Y_{mtE/m}$		mt-yield per tissues mass; $Y_{mtE/m} = Y_{mtE} \cdot D_{mtE}$
1469				
1470	molar format	\underline{n}	[mol]	Table 6
1471	negative	neg		Figure 3
1472	number concentration of X	C_{NX}	[x·m ⁻³]	Table 4
1473	number format	\underline{N}	[x]	Table 4, Figure 7
1474	number of entities X	N_X	[x]	Table 4, Figure 7
1475	number of entity B	N_B	[x]	Table 4
1476	oxidative phosphorylation	OXPHOS		state; Table 1, Figure 5
1477	oxygen concentration	$c_{O_2} = n_{O_2} \cdot V^{-1}$	[mol·m ⁻³]	[O ₂]; Section 3.2
1478	oxygen flux, in reaction r	J_{rO_2}	<i>varies</i>	Figure 1
1479	pathway control state	PCS		##
1480	permeabilized cell number	N_{pce}	[x]	experimental permeabilization of plasma membrane; Table 5
1481				
1482	phosphorylation of ADP to ATP	P»		Section 2.2
1483	P»/O ₂ ratio	P»/O ₂		mechanistic $Y_{P»/O_2}$, calculated from pump stoichiometries; Figure 2B
1484				
1485	positive	pos		Figure 3
1486	proton in the negative compartment	H ⁺ _{neg}		Figure 3
1487	proton in the positive compartment	H ⁺ _{pos}		Figure 3
1488	rate of electron transfer in ET state	E		ET-capacity; Table 1
1489	rate of LEAK respiration	L		Table 1
1490	rate of oxidative phosphorylation	P		OXPHOS capacity; Table 1
1491	rate of residual oxygen consumption	Rox		Table 1, Figure 1
1492	residual oxygen consumption	ROX		state; Table 1
1493	respiratory supercomplex	SC I _n III _n IV _n		supramolecular assemblies composed of variable copy numbers (n) of CI, CIII and CIV; Box 1
1494				
1495				
1496	specific mitochondrial density	$D_{mtE} = mtE \cdot m_X^{-1}$	[mtEU·kg ⁻¹]	Table 4
1497	substrate-uncoupler-inhibitor-			

1498	titration protocol	SUIT		##
1499	volume	V	$[m^{-3}]$	Table 7
1500	volume format	\underline{V}	$[m^{-3}]$	Table 6

1502
 1503 Experimentally, respiration is separated in mitochondrial preparations from the interactions with
 1504 the fermentative pathways of the intact cell. OXPHOS analysis (**Figure 3**) is based on the study of
 1505 mitochondrial preparations complementary to bioenergetic investigations of intact cells and
 1506 organisms—from model organisms to the human species including healthy and diseased persons
 1507 (patients). Different mechanisms of respiratory uncoupling have to be distinguished (**Figure 4**).
 1508 Metabolic fluxes measured in defined coupling and pathway control states (**Figures 5 and 6**) provide
 1509 insights into the meaning of cellular and organismic respiration.

1510 The optimal choice for expressing mitochondrial and cell respiration as O_2 flow per biological
 1511 sample, and normalization for specific tissue-markers (volume, mass, protein) and mitochondrial
 1512 markers (volume, protein, content, mtDNA, activity of marker enzymes, respiratory reference state) is
 1513 guided by the scientific question under study. Interpretation of the data depends critically on appropriate
 1514 normalization (**Figure 7**).

1515 MitoEAGLE can serve as a gateway to better diagnose mitochondrial respiratory adaptations and
 1516 defects linked to genetic variation, age-related health risks, sex-specific mitochondrial performance,
 1517 lifestyle with its effects on degenerative diseases, and thermal and chemical environment. The present
 1518 recommendations on coupling control states and rates, linked to the concept of the protonmotive force,
 1519 are focused on studies with mitochondrial preparations (**Box 3**). These will be extended in a series of
 1520 reports on pathway control of mitochondrial respiration, respiratory states in intact cells, and
 1521 harmonization of experimental procedures.

1522 **Acknowledgements**

1523 We thank M. Beno for management assistance. This publication is based upon work from COST Action
 1524 CA15203 MitoEAGLE, supported by COST (European Cooperation in Science and Technology), and
 1525 K-Regio project MitoFit (E.G.).

1526
 1527 **Competing financial interests:** E.G. is founder and CEO of Oroboros Instruments, Innsbruck, Austria.

1528 **References**

- 1529
 1530
 1531
 1532 Altmann R (1894) Die Elementarorganismen und ihre Beziehungen zu den Zellen. Zweite vermehrte Auflage.
 1533 Verlag Von Veit & Comp, Leipzig:160 pp.
 1534 Baggeto LG, Testa-Perussini R (1990) Role of acetoin on the regulation of intermediate metabolism of Ehrlich
 1535 ascites tumor mitochondria: its contribution to membrane cholesterol enrichment modifying passive proton
 1536 permeability. Arch Biochem Biophys 283:341-8.
 1537 Beard DA (2005) A biophysical model of the mitochondrial respiratory system and oxidative phosphorylation.
 1538 PLoS Comput Biol 1(4):e36.
 1539 Benda C (1898) Weitere Mitteilungen über die Mitochondria. Verh Dtsch Physiol Ges:376-83.
 1540 Birkedal R, Laasmaa M, Vendelin M (2014) The location of energetic compartments affects energetic
 1541 communication in cardiomyocytes. Front Physiol 5:376.
 1542 Blier PU, Dufresne F, Burton RS (2001) Natural selection and the evolution of mtDNA-encoded peptides:
 1543 evidence for intergenomic co-adaptation. Trends Genet 17:400-6.
 1544 Blier PU, Guderley HE (1993) Mitochondrial activity in rainbow trout red muscle: the effect of temperature on
 1545 the ADP-dependence of ATP synthesis. J Exp Biol 176:145-58.
 1546 Breton S, Beaupré HD, Stewart DT, Hoeh WR, Blier PU (2007) The unusual system of doubly uniparental
 1547 inheritance of mtDNA: isn't one enough? Trends Genet 23:465-74.
 1548 Brown GC (1992) Control of respiration and ATP synthesis in mammalian mitochondria and cells. Biochem J
 1549 284:1-13.
 1550 Burger G, Gray MW, Forget L, Lang BF (2013) Strikingly bacteria-like and gene-rich mitochondrial genomes
 1551 throughout jakobid protists. Genome Biol Evol 5:418-38.
 1552 Calvo SE, Klauser CR, Mootha VK (2016) MitoCarta2.0: an updated inventory of mammalian mitochondrial
 1553 proteins. Nucleic Acids Research 44:D1251-7.
 1554 Calvo SE, Julien O, Clauser KR, Shen H, Kamer KJ, Wells JA, Mootha VK (2017) Comparative analysis of
 1555 mitochondrial N-termini from mouse, human, and yeast. Mol Cell Proteomics 16:512-23.

- 1556 Campos JC, Queliconi BB, Bozi LHM, Bechara LRG, Dourado PMM, Andres AM, Jannig PR, Gomes KMS,
 1557 Zambelli VO, Rocha-Resende C, Guatimosim S, Brum PC, Mochly-Rosen D, Gottlieb RA, Kowaltowski AJ,
 1558 Ferreira JCB (2017) Exercise reestablishes autophagic flux and mitochondrial quality control in heart failure.
 1559 *Autophagy* 13:1304-317.
- 1560 Canton M, Luvisetto S, Schmehl I, Azzone GF (1995) The nature of mitochondrial respiration and
 1561 discrimination between membrane and pump properties. *Biochem J* 310:477-81.
- 1562 Carrico C, Meyer JG, He W, Gibson BW, Verdin E (2018) The mitochondrial acylome emerges: proteomics,
 1563 regulation by Sirtuins, and metabolic and disease implications. *Cell Metab* 27:497-512.
- 1564 Chan DC (2006) Mitochondria: dynamic organelles in disease, aging, and development. *Cell* 125:1241-52.
- 1565 Chance B, Williams GR (1955a) Respiratory enzymes in oxidative phosphorylation. I. Kinetics of oxygen
 1566 utilization. *J Biol Chem* 217:383-93.
- 1567 Chance B, Williams GR (1955b) Respiratory enzymes in oxidative phosphorylation: III. The steady state. *J Biol*
 1568 *Chem* 217:409-27.
- 1569 Chance B, Williams GR (1955c) Respiratory enzymes in oxidative phosphorylation. IV. The respiratory chain. *J*
 1570 *Biol Chem* 217:429-38.
- 1571 Chance B, Williams GR (1956) The respiratory chain and oxidative phosphorylation. *Adv Enzymol Relat Subj*
 1572 *Biochem* 17:65-134.
- 1573 Chowdhury SK, Djordjevic J, Albensi B, Fernyhough P (2015) Simultaneous evaluation of substrate-dependent
 1574 oxygen consumption rates and mitochondrial membrane potential by TMRM and safranin in cortical
 1575 mitochondria. *Biosci Rep* 36:e00286.
- 1576 Cobb LJ, Lee C, Xiao J, Yen K, Wong RG, Nakamura HK, Mehta HH, Gao Q, Ashur C, Huffman DM, Wan J,
 1577 Muzumdar R, Barzilai N, Cohen P (2016) Naturally occurring mitochondrial-derived peptides are age-
 1578 dependent regulators of apoptosis, insulin sensitivity, and inflammatory markers. *Aging (Albany NY)* 8:796-
 1579 809.
- 1580 Cohen ER, Cvitas T, Frey JG, Holmström B, Kuchitsu K, Marquardt R, Mills I, Pavese F, Quack M, Stohner J,
 1581 Strauss HL, Takami M, Thor HL (2008) Quantities, units and symbols in physical chemistry, IUPAC Green
 1582 Book, 3rd Edition, 2nd Printing, IUPAC & RSC Publishing, Cambridge.
- 1583 Cooper H, Hedges LV, Valentine JC, eds (2009) *The handbook of research synthesis and meta-analysis*. Russell
 1584 Sage Foundation.
- 1585 Coopersmith J (2010) Energy, the subtle concept. The discovery of Feynman's blocks from Leibnitz to Einstein.
 1586 Oxford University Press:400 pp.
- 1587 Cummins J (1998) Mitochondrial DNA in mammalian reproduction. *Rev Reprod* 3:172-82.
- 1588 Dai Q, Shah AA, Garde RV, Yonish BA, Zhang L, Medvitz NA, Miller SE, Hansen EL, Dunn CN, Price TM
 1589 (2013) A truncated progesterone receptor (PR-M) localizes to the mitochondrion and controls cellular
 1590 respiration. *Mol Endocrinol* 27:741-53.
- 1591 Daum B, Walter A, Horst A, Osiewacz HD, Kühlbrandt W (2013) Age-dependent dissociation of ATP synthase
 1592 dimers and loss of inner-membrane cristae in mitochondria. *Proc Natl Acad Sci U S A* 110:15301-6.
- 1593 Divakaruni AS, Brand MD (2011) The regulation and physiology of mitochondrial proton leak. *Physiology*
 1594 (Bethesda) 26:192-205.
- 1595 Doerrier C, Garcia-Souza LF, Krumschnabel G, Wohlfarter Y, Mészáros AT, Gnaiger E (2018) High-Resolution
 1596 FluoRespirometry and OXPHOS protocols for human cells, permeabilized fibres from small biopsies of
 1597 muscle, and isolated mitochondria. *Methods Mol Biol* 1782 (Palmeira CM, Moreno AJ, eds): Mitochondrial
 1598 Bioenergetics, 978-1-4939-7830-4.
- 1599 Doskey CM, van 't Erve TJ, Wagner BA, Buettner GR (2015) Moles of a substance per cell is a highly
 1600 informative dosing metric in cell culture. *PLOS ONE* 10:e0132572.
- 1601 Drahotová Z, Milerová M, Stieglerová A, Houstek J, Ostádal B (2004) Developmental changes of cytochrome *c*
 1602 oxidase and citrate synthase in rat heart homogenate. *Physiol Res* 53:119-22.
- 1603 Duarte FV, Palmeira CM, Rolo AP (2014) The role of microRNAs in mitochondria: small players acting wide.
 1604 *Genes (Basel)* 5:865-86.
- 1605 Ehinger JK, Morota S, Hansson MJ, Paul G, Elmér E (2015) Mitochondrial dysfunction in blood cells from
 1606 amyotrophic lateral sclerosis patients. *J Neurol* 262:1493-503.
- 1607 Ernster L, Schatz G (1981) Mitochondria: a historical review. *J Cell Biol* 91:227s-55s.
- 1608 Estabrook RW (1967) Mitochondrial respiratory control and the polarographic measurement of ADP:O ratios.
 1609 *Methods Enzymol* 10:41-7.
- 1610 Faber C, Zhu ZJ, Castellino S, Wagner DS, Brown RH, Peterson RA, Gates L, Barton J, Bickett M, Hagerty L,
 1611 Kimbrough C, Sola M, Bailey D, Jordan H, Elangbam CS (2014) Cardiolipin profiles as a potential
 1612 biomarker of mitochondrial health in diet-induced obese mice subjected to exercise, diet-restriction and
 1613 ephedrine treatment. *J Appl Toxicol* 34:1122-9.
- 1614 Feagin JE, Harrell MI, Lee JC, Coe KJ, Sands BH, Cannone JJ, Tami G, Schnare MN, Gutell RR (2012) The
 1615 fragmented mitochondrial ribosomal RNAs of *Plasmodium falciparum*. *PLoS One* 7:e38320.
- 1616 Fell D (1997) *Understanding the control of metabolism*. Portland Press.

- 1617 Forstner H, Gnaiger E (1983) Calculation of equilibrium oxygen concentration. In: Polarographic Oxygen
 1618 Sensors. Aquatic and Physiological Applications. Gnaiger E, Forstner H (eds), Springer, Berlin, Heidelberg,
 1619 New York:321-33.
- 1620 Garlid KD, Beavis AD, Ratkje SK (1989) On the nature of ion leaks in energy-transducing membranes. *Biochim*
 1621 *Biophys Acta* 976:109-20.
- 1622 Garlid KD, Semrad C, Zinchenko V. Does redox slip contribute significantly to mitochondrial respiration? In:
 1623 Schuster S, Rigoulet M, Ouhabi R, Mazat J-P, eds (1993) *Modern trends in biothermokinetics*. Plenum Press,
 1624 New York, London:287-93.
- 1625 Gerö D, Szabo C (2016) Glucocorticoids suppress mitochondrial oxidant production via upregulation of
 1626 uncoupling protein 2 in hyperglycemic endothelial cells. *PLoS One* 11:e0154813.
- 1627 Gnaiger E. Efficiency and power strategies under hypoxia. Is low efficiency at high glycolytic ATP production a
 1628 paradox? In: *Surviving Hypoxia: Mechanisms of Control and Adaptation*. Hochachka PW, Lutz PL, Sick T,
 1629 Rosenthal M, Van den Thillart G, eds (1993a) CRC Press, Boca Raton, Ann Arbor, London, Tokyo:77-109.
- 1630 Gnaiger E (1993b) Nonequilibrium thermodynamics of energy transformations. *Pure Appl Chem* 65:1983-2002.
- 1631 Gnaiger E (2001) Bioenergetics at low oxygen: dependence of respiration and phosphorylation on oxygen and
 1632 adenosine diphosphate supply. *Respir Physiol* 128:277-97.
- 1633 Gnaiger E (2009) Capacity of oxidative phosphorylation in human skeletal muscle. New perspectives of
 1634 mitochondrial physiology. *Int J Biochem Cell Biol* 41:1837-45.
- 1635 Gnaiger E (2014) Mitochondrial pathways and respiratory control. An introduction to OXPHOS analysis. 4th ed.
 1636 *Mitochondr Physiol Network* 19.12. Oroboros MiPNet Publications, Innsbruck:80 pp.
- 1637 Gnaiger E, Méndez G, Hand SC (2000) High phosphorylation efficiency and depression of uncoupled respiration
 1638 in mitochondria under hypoxia. *Proc Natl Acad Sci USA* 97:11080-5.
- 1639 Greggio C, Jha P, Kulkarni SS, Lagarrigue S, Broskey NT, Boutant M, Wang X, Conde Alonso S, Ofori E,
 1640 Auwerx J, Cantó C, Amati F (2017) Enhanced respiratory chain supercomplex formation in response to
 1641 exercise in human skeletal muscle. *Cell Metab* 25:301-11.
- 1642 Hinkle PC (2005) P/O ratios of mitochondrial oxidative phosphorylation. *Biochim Biophys Acta* 1706:1-11.
- 1643 Hofstadter DR (1979) Gödel, Escher, Bach: An eternal golden braid. A metaphorical fugue on minds and
 1644 machines in the spirit of Lewis Carroll. Harvester Press:499 pp.
- 1645 Illaste A, Laasmaa M, Peterson P, Vendelin M (2012) Analysis of molecular movement reveals latticelike
 1646 obstructions to diffusion in heart muscle cells. *Biophys J* 102:739-48.
- 1647 Jasienski M, Bazzaz FA (1999) The fallacy of ratios and the testability of models in biology. *Oikos* 84:321-26.
- 1648 Jepihhina N, Beraud N, Sepp M, Birkedal R, Vendelin M (2011) Permeabilized rat cardiomyocyte response
 1649 demonstrates intracellular origin of diffusion obstacles. *Biophys J* 101:2112-21.
- 1650 Karnkowska A, Vacek V, Zubáčová Z, Treitli SC, Petrželková R, Eme L, Novák L, Žárský V, Barlow LD,
 1651 Herman EK, Soukal P, Hroudová M, Doležal P, Stairs CW, Roger AJ, Eliáš M, Dacks JB, Vlček Č, Hampl V
 1652 (2016) A eukaryote without a mitochondrial organelle. *Curr Biol* 26:1274-84.
- 1653 Klepinin A, Ounpuu L, Guzun R, Chekulayev V, Timohhina N, Tepp K, Shevchuk I, Schlattner U, Kaambre T
 1654 (2016) Simple oxygraphic analysis for the presence of adenylate kinase 1 and 2 in normal and tumor cells. *J*
 1655 *Bioenerg Biomembr* 48:531-48.
- 1656 Klingenberg M (2017) UCP1 - A sophisticated energy valve. *Biochimie* 134:19-27.
- 1657 Koit A, Shevchuk I, Ounpuu L, Klepinin A, Chekulayev V, Timohhina N, Tepp K, Puurand M, Truu L, Heck K,
 1658 Valvere V, Guzun R, Kaambre T (2017) Mitochondrial respiration in human colorectal and breast cancer
 1659 clinical material is regulated differently. *Oxid Med Cell Longev* 1372640.
- 1660 Komlódi T, Tretter L (2017) Methylene blue stimulates substrate-level phosphorylation catalysed by succinyl-
 1661 CoA ligase in the citric acid cycle. *Neuropharmacology* 123:287-98.
- 1662 Korn E (1969) Cell membranes: structure and synthesis. *Annu Rev Biochem* 38:263-88.
- 1663 Lai N, M Kummitha C, Rosca MG, Fujioka H, Tandler B, Hoppel CL (2018) Isolation of mitochondrial
 1664 subpopulations from skeletal muscle: optimizing recovery and preserving integrity. *Acta Physiol*
 1665 (Oxf):e13182. doi: 10.1111/apha.13182.
- 1666 Lane N (2005) *Power, sex, suicide: mitochondria and the meaning of life*. Oxford University Press:354 pp.
- 1667 Larsen S, Nielsen J, Neigaard Nielsen C, Nielsen LB, Wibrand F, Stride N, Schroder HD, Boushel RC, Helge
 1668 JW, Dela F, Hey-Mogensen M (2012) Biomarkers of mitochondrial content in skeletal muscle of healthy
 1669 young human subjects. *J Physiol* 590:3349-60.
- 1670 Lee C, Zeng J, Drew BG, Sallam T, Martin-Montalvo A, Wan J, Kim SJ, Mehta H, Hevener AL, de Cabo R,
 1671 Cohen P (2015) The mitochondrial-derived peptide MOTS-c promotes metabolic homeostasis and reduces
 1672 obesity and insulin resistance. *Cell Metab* 21:443-54.
- 1673 Lee SR, Kim HK, Song IS, Youm J, Dizon LA, Jeong SH, Ko TH, Heo HJ, Ko KS, Rhee BD, Kim N, Han J
 1674 (2013) Glucocorticoids and their receptors: insights into specific roles in mitochondria. *Prog Biophys Mol*
 1675 *Biol* 112:44-54.
- 1676 Leek BT, Mudaliar SR, Henry R, Mathieu-Costello O, Richardson RS (2001) Effect of acute exercise on citrate
 1677 synthase activity in untrained and trained human skeletal muscle. *Am J Physiol Regul Integr Comp Physiol*
 1678 280:R441-7.

- 1679 Lemieux H, Blier PU, Gnaiger E (2017) Remodeling pathway control of mitochondrial respiratory capacity by
 1680 temperature in mouse heart: electron flow through the Q-junction in permeabilized fibers. *Sci Rep* 7:2840.
 1681 Lenaz G, Tioli G, Falasca AI, Genova ML (2017) Respiratory supercomplexes in mitochondria. In: *Mechanisms*
 1682 *of primary energy trasduction in biology*. M Wikstrom (ed) Royal Society of Chemistry Publishing, London,
 1683 UK:296-337.
- 1684 Liu S, Roellig DM, Guo Y, Li N, Frace MA, Tang K, Zhang L, Feng Y, Xiao L (2016) Evolution of mitosome
 1685 metabolism and invasion-related proteins in *Cryptosporidium*. *BMC Genomics* 17:1006.
- 1686 Margulis L (1970) *Origin of eukaryotic cells*. New Haven: Yale University Press.
- 1687 Meinild Lundby AK, Jacobs RA, Gehrig S, de Leur J, Hauser M, Bonne TC, Flück D, Dandanell S, Kirk N,
 1688 Kaech A, Ziegler U, Larsen S, Lundby C (2018) Exercise training increases skeletal muscle mitochondrial
 1689 volume density by enlargement of existing mitochondria and not de novo biogenesis. *Acta Physiol* 222,
 1690 e12905.
- 1691 Menshikova EV, Ritov VB, Fairfull L, Ferrell RE, Kelley DE, Goodpaster BH (2006) Effects of exercise on
 1692 mitochondrial content and function in aging human skeletal muscle. *J Gerontol A Biol Sci Med Sci* 61:534-
 1693 40.
- 1694 Menshikova EV, Ritov VB, Ferrell RE, Azuma K, Goodpaster BH, Kelley DE (2007) Characteristics of skeletal
 1695 muscle mitochondrial biogenesis induced by moderate-intensity exercise and weight loss in obesity. *J Appl*
 1696 *Physiol* (1985) 103:21-7.
- 1697 Menshikova EV, Ritov VB, Toledo FG, Ferrell RE, Goodpaster BH, Kelley DE (2005) Effects of weight loss
 1698 and physical activity on skeletal muscle mitochondrial function in obesity. *Am J Physiol Endocrinol Metab*
 1699 288:E818-25.
- 1700 Miller GA (1991) *The science of words*. Scientific American Library New York:276 pp.
- 1701 Mitchell P (1961) Coupling of phosphorylation to electron and hydrogen transfer by a chemi-osmotic type of
 1702 mechanism. *Nature* 191:144-8.
- 1703 Mitchell P (2011) Chemiosmotic coupling in oxidative and photosynthetic phosphorylation. *Biochim Biophys*
 1704 *Acta Bioenergetics* 1807:1507-38.
- 1705 Mogensen M, Sahlin K, Fernström M, Glintborg D, Vind BF, Beck-Nielsen H, Højlund K (2007) Mitochondrial
 1706 respiration is decreased in skeletal muscle of patients with type 2 diabetes. *Diabetes* 56:1592-9.
- 1707 Mohr PJ, Phillips WD (2015) Dimensionless units in the SI. *Metrologia* 52:40-7.
- 1708 Moreno M, Giacco A, Di Munno C, Goglia F (2017) Direct and rapid effects of 3,5-diiodo-L-thyronine (T2).
 1709 *Mol Cell Endocrinol* 7207:30092-8.
- 1710 Morrow RM, Picard M, Derbeneva O, Leipzig J, McManus MJ, Gouspillou G, Barbat-Artigas S, Dos Santos C,
 1711 Hepple RT, Murdock DG, Wallace DC (2017) Mitochondrial energy deficiency leads to hyperproliferation of
 1712 skeletal muscle mitochondria and enhanced insulin sensitivity. *Proc Natl Acad Sci U S A* 114:2705-10.
- 1713 Murley A, Nunnari J (2016) The emerging network of mitochondria-organelle contacts. *Mol Cell* 61:648-53.
- 1714 National Academies of Sciences, Engineering, and Medicine (2018) *International coordination for science data*
 1715 *infrastructure: Proceedings of a workshop—in brief*. Washington, DC: The National Academies Press. doi:
 1716 <https://doi.org/10.17226/25015>.
- 1717 Oemer G, Lackner L, Muigg K, Krumschnabel G, Watschinger K, Sailer S, Lindner H, Gnaiger E, Wortmann
 1718 SB, Werner ER, Zschocke J, Keller MA (2018) The molecular structural diversity of mitochondrial
 1719 cardiolipins. *Proc Nat Acad Sci U S A* 115:4158-63.
- 1720 Palmfeldt J, Bross P (2017) Proteomics of human mitochondria. *Mitochondrion* 33:2-14.
- 1721 Paradies G, Paradies V, De Benedictis V, Ruggiero FM, Petrosillo G (2014) Functional role of cardiolipin in
 1722 mitochondrial bioenergetics. *Biochim Biophys Acta* 1837:408-17.
- 1723 Pesta D, Gnaiger E (2012) High-Resolution Respirometry. OXPHOS protocols for human cells and
 1724 permeabilized fibres from small biopsies of human muscle. *Methods Mol Biol* 810:25-58.
- 1725 Pesta D, Hoppel F, Macek C, Messner H, Faulhaber M, Kobel C, Parson W, Burtscher M, Schocke M, Gnaiger
 1726 E (2011) Similar qualitative and quantitative changes of mitochondrial respiration following strength and
 1727 endurance training in normoxia and hypoxia in sedentary humans. *Am J Physiol Regul Integr Comp Physiol*
 1728 301:R1078–87.
- 1729 Price TM, Dai Q (2015) The role of a mitochondrial progesterone receptor (PR-M) in progesterone action.
 1730 *Semin Reprod Med* 33:185-94.
- 1731 Puchowicz MA, Varnes ME, Cohen BH, Friedman NR, Kerr DS, Hoppel CL (2004) Oxidative phosphorylation
 1732 analysis: assessing the integrated functional activity of human skeletal muscle mitochondria – case studies.
 1733 *Mitochondrion* 4:377-85. Puntchart A, Claassen H, Jostarndt K, Hoppeler H, Billeter R (1995) mRNAs of
 1734 enzymes involved in energy metabolism and mtDNA are increased in endurance-trained athletes. *Am J*
 1735 *Physiol* 269:C619-25.
- 1736 Quiros PM, Mottis A, Auwerx J (2016) Mitonuclear communication in homeostasis and stress. *Nat Rev Mol*
 1737 *Cell Biol* 17:213-26.
- 1738 Rackham O, Mercer TR, Filipovska A (2012) The human mitochondrial transcriptome and the RNA-binding
 1739 proteins that regulate its expression. *WIREs RNA* 3:675–95.

- 1740 Reichmann H, Hoppeler H, Mathieu-Costello O, von Bergen F, Pette D (1985) Biochemical and ultrastructural
 1741 changes of skeletal muscle mitochondria after chronic electrical stimulation in rabbits. *Pflugers Arch* 404:1-
 1742 9.
- 1743 Renner K, Amberger A, Konwalinka G, Gnaiger E (2003) Changes of mitochondrial respiration, mitochondrial
 1744 content and cell size after induction of apoptosis in leukemia cells. *Biochim Biophys Acta* 1642:115-23.
- 1745 Rice DW, Alverson AJ, Richardson AO, Young GJ, Sanchez-Puerta MV, Munzinger J, Barry K, Boore JL,
 1746 Zhang Y, dePamphilis CW, Knox EB, Palmer JD (2016) Horizontal transfer of entire genomes via
 1747 mitochondrial fusion in the angiosperm *Amborella*. *Science* 342:1468-73.
- 1748 Rich P (2003) Chemiosmotic coupling: The cost of living. *Nature* 421:583.
- 1749 Rich PR (2013) Chemiosmotic theory. *Encyclopedia Biol Chem* 1:467-72.
- 1750 Roger JA, Munoz-Gomes SA, Kamikawa R (2017) The origin and diversification of mitochondria. *Curr Biol*
 1751 27:R1177-92.
- 1752 Rostovtseva TK, Sheldon KL, Hassanzadeh E, Monge C, Saks V, Bezrukov SM, Sackett DL (2008) Tubulin
 1753 binding blocks mitochondrial voltage-dependent anion channel and regulates respiration. *Proc Natl Acad Sci*
 1754 USA 105:18746-51.
- 1755 Rustin P, Parfait B, Chretien D, Bourgeron T, Djouadi F, Bastin J, Rötig A, Munnich A (1996) Fluxes of
 1756 nicotinamide adenine dinucleotides through mitochondrial membranes in human cultured cells. *J Biol Chem*
 1757 271:14785-90.
- 1758 Saks VA, Veksler VI, Kuznetsov AV, Kay L, Sikk P, Tiivel T, Tranqui L, Olivares J, Winkler K, Wiedemann F,
 1759 Kunz WS (1998) Permeabilised cell and skinned fiber techniques in studies of mitochondrial function in
 1760 vivo. *Mol Cell Biochem* 184:81-100.
- 1761 Salabei JK, Gibb AA, Hill BG (2014) Comprehensive measurement of respiratory activity in permeabilized cells
 1762 using extracellular flux analysis. *Nat Protoc* 9:421-38.
- 1763 Sazanov LA (2015) A giant molecular proton pump: structure and mechanism of respiratory complex I. *Nat Rev*
 1764 Mol Cell Biol 16:375-88.
- 1765 Schneider TD (2006) Claude Shannon: biologist. The founder of information theory used biology to formulate
 1766 the channel capacity. *IEEE Eng Med Biol Mag* 25:30-3.
- 1767 Schönfeld P, Dymkowska D, Wojtczak L (2009) Acyl-CoA-induced generation of reactive oxygen species in
 1768 mitochondrial preparations is due to the presence of peroxisomes. *Free Radic Biol Med* 47:503-9.
- 1769 Schultz J, Wiesner RJ (2000) Proliferation of mitochondria in chronically stimulated rabbit skeletal muscle--
 1770 transcription of mitochondrial genes and copy number of mitochondrial DNA. *J Bioenerg Biomembr* 32:627-
 1771 34.
- 1772 Speijer D (2016) Being right on Q: shaping eukaryotic evolution. *Biochem J* 473:4103-27.
- 1773 Sugiura A, Mattie S, Prudent J, McBride HM (2017) Newly born peroxisomes are a hybrid of mitochondrial and
 1774 ER-derived pre-peroxisomes. *Nature* 542:251-4.
- 1775 Simson P, Jepihhina N, Laasmaa M, Peterson P, Birkedal R, Vendelin M (2016) Restricted ADP movement in
 1776 cardiomyocytes: Cytosolic diffusion obstacles are complemented with a small number of open mitochondrial
 1777 voltage-dependent anion channels. *J Mol Cell Cardiol* 97:197-203.
- 1778 Stucki JW, Ineichen EA (1974) Energy dissipation by calcium recycling and the efficiency of calcium transport
 1779 in rat-liver mitochondria. *Eur J Biochem* 48:365-75.
- 1780 Tonkonogi M, Harris B, Sahlin K (1997) Increased activity of citrate synthase in human skeletal muscle after a
 1781 single bout of prolonged exercise. *Acta Physiol Scand* 161:435-6.
- 1782 Torralba D, Baixauli F, Sánchez-Madrid F (2016) Mitochondria know no boundaries: mechanisms and functions
 1783 of intercellular mitochondrial transfer. *Front Cell Dev Biol* 4:107. eCollection 2016.
- 1784 Vamecq J, Schepers L, Parmentier G, Mannaerts GP (1987) Inhibition of peroxisomal fatty acyl-CoA oxidase by
 1785 antimycin A. *Biochem J* 248:603-7.
- 1786 Waczulikova I, Habodaszova D, Cagalinec M, Ferko M, Ulicna O, Mateasik A, Sikurova L, Ziegelhöffer A
 1787 (2007) Mitochondrial membrane fluidity, potential, and calcium transients in the myocardium from acute
 1788 diabetic rats. *Can J Physiol Pharmacol* 85:372-81.
- 1789 Wagner BA, Venkataraman S, Buettner GR (2011) The rate of oxygen utilization by cells. *Free Radic Biol Med*
 1790 51:700-712.
- 1791 Wang H, Hiatt WR, Barstow TJ, Brass EP (1999) Relationships between muscle mitochondrial DNA content,
 1792 mitochondrial enzyme activity and oxidative capacity in man: alterations with disease. *Eur J Appl Physiol*
 1793 Occup Physiol 80:22-7.
- 1794 Watt IN, Montgomery MG, Runswick MJ, Leslie AG, Walker JE (2010) Bioenergetic cost of making an
 1795 adenosine triphosphate molecule in animal mitochondria. *Proc Natl Acad Sci U S A* 107:16823-7.
- 1796 Weibel ER, Hoppeler H (2005) Exercise-induced maximal metabolic rate scales with muscle aerobic capacity. *J*
 1797 *Exp Biol* 208:1635-44.
- 1798 White DJ, Wolff JN, Pierson M, Gemmill NJ (2008) Revealing the hidden complexities of mtDNA inheritance.
 1799 *Mol Ecol* 17:4925-42.
- 1800 Wikström M, Hummer G (2012) Stoichiometry of proton translocation by respiratory complex I and its
 1801 mechanistic implications. *Proc Natl Acad Sci U S A* 109:4431-6.

- 1802 Williams EG, Wu Y, Jha P, Dubuis S, Blattmann P, Argmann CA, Houten SM, Amariuta T, Wolski W,
 1803 Zamboni N, Aebersold R, Auwerx J (2016) Systems proteomics of liver mitochondria function. *Science* 352
 1804 (6291):aad0189
- 1805 Willis WT, Jackman MR, Messer JI, Kuzmiak-Glancy S, Glancy B (2016) A simple hydraulic analog model of
 1806 oxidative phosphorylation. *Med Sci Sports Exerc* 48:990-1000.
- 1807 Zíková A, Hampl V, Paris Z, Týč J, Lukeš J (2016) Aerobic mitochondria of parasitic protists: diverse genomes
 1808 and complex functions. *Mol Biochem Parasitol* 209:46-57.

1810 Supplement

1811

1812 Manuscript phases and versions - an open-access approach

1813

1814 This manuscript on ‘Mitochondrial respiratory states and rates’ is a position statement in the frame of COST Action
 1815 CA15203 MitoEAGLE. The list of co-authors evolved beyond phase 1 in the bottom-up spirit of COST.

1816 The global MitoEAGLE network made it possible to collaborate with a large number of co-authors to reach
 1817 consensus on the present manuscript. Nevertheless, we do not consider scientific progress to be supported by
 1818 ‘declaration’ statements (other than on ethical or political issues). Our manuscript aims at providing arguments for
 1819 further debate rather than pushing opinions. We hope to initiate a much broader process of discussion and want to
 1820 raise the awareness on the importance of a consistent terminology for reporting of scientific data in the field of
 1821 bioenergetics, mitochondrial physiology and pathology. Quality of research requires quality of communication.
 1822 Some established researchers in the field may not want to re-consider the use of jargon which has become
 1823 established despite deficiencies of accuracy and meaning. In the long run, superior standards will become accepted.
 1824 We hope to contribute to this evolutionary process, with an emphasis on harmonization rather than standardization.

1825 *Phase 1* The protonmotive force and respiratory control

1826 http://www.mitoeagle.org/index.php/The_protonmotive_force_and_respiratory_control

1827 • 2017-04-09 to 2017-09-18 (44 versions)

1828 • 2017-09-21 to 2018-02-06 (21 versions)

1829 http://www.mitoeagle.org/index.php/MitoEAGLE_preprint_2017-09-21

1830 2017-11-11: Print version (16) for MiP2017/MitoEAGLE conference in Hradec Kralove

1831 *Phase 2* Mitochondrial respiratory states and rates: Building blocks of mitochondrial physiology Part 1

1832 http://www.mitoeagle.org/index.php/MitoEAGLE_preprint_2018-02-08

1833 • 2018-02-08 – (42 Versions up to 2018-09-24)

1834 *Phase 3* Submission to a preprint server: [BioRxiv](https://www.biorxiv.org/)

1835 *Phase 4* Journal submission

1836 CELL METABOLISM, aiming at indexing by *The Web of Science* and *PubMed*. We expect feedback from
 1837 many colleagues until the end of May, to prepare a final circular to all co-authors in June 2018.

1838

1839 Authors

1840

1841 This manuscript developed as an open invitation to scientists and students to join as co-authors, to provide a
 1842 balanced view on mitochondrial respiratory control and a consensus statement on reporting data of mitochondrial
 1843 respiration in terms of metabolic flows and fluxes.

1844 Co-authors are added in alphabetical order based upon a first draft written by the corresponding author, who
 1845 edited all versions. *Co-authors confirm to have read the final manuscript, possibly have made additions or*
 1846 *suggestions for improvement, and agree to implement the recommendations into future manuscripts, presentations*
 1847 *and teaching materials.*

1848 We continue to invite comments and suggestions, particularly if you are an early career investigator adding
 1849 an open future-oriented perspective, or an established scientist providing a balanced historical basis. Your critical
 1850 input into the quality of the manuscript will be most welcome, improving our aims to be educational, general,
 1851 consensus-oriented, and practically helpful for students working in mitochondrial respiratory physiology.

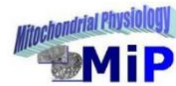
1852 To join as a co-author, please feel free to focus on a particular section, providing direct input and references,
 1853 and contributing to the scope of the manuscript from the perspective of your expertise. Your comments will be
 1854 largely posted on the discussion page of the MitoEAGLE preprint website.

1855 If you prefer to submit comments in the format of a referee's evaluation rather than a contribution as a co-
 1856 author, we will be glad to distribute your views to the updated list of co-authors for a balanced response. We would
 1857 ask for your consent on this open bottom-up policy.

1858



Mitochondrial respiratory states and rates:



Building blocks of mitochondrial physiology

Part 1 - www.mitoeagle.org/index.php/MitoEAGLE_preprint_2018-02-08

Gnaiger E^{1,2}, corresponding author
355 co-authors, MitoEAGLE Working Group

¹Medical University Innsbruck
²Oroboros, Innsbruck, Austria

Aims Clarity of concept and consistency of nomenclature facilitate effective transdisciplinary communication, education, and ultimately further discovery.

Adhering to uniform standards and harmonizing the terminology concerning mitochondrial respiratory states and rates will support the development of databases of mitochondrial respiratory function in cells, tissues, and species.

Summary Recommendations on coupling control states and rates are focused on studies with mitochondrial preparations.

- Fig. 1:** Respiration is defined by O₂ flux balance.
- Fig. 2:** OXPHOS analysis is based on the study of mt- preparations. Metabolic fluxes measured in defined coupling and pathway control states provide insights into the meaning of cellular respiration.
- Fig. 3:** Interpretation of respiratory rates depends critically on appropriate normalization.

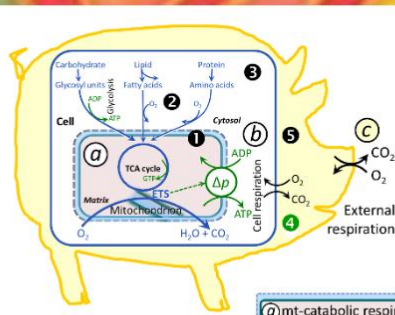
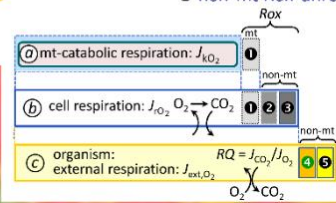


Figure 1. From mitochondrial to external respiration

Mitochondrial (mt) respiration is the oxidation of fuel substrates (electron donors) and reduction of O₂ catalysed by the electron transfer system, ETS:

- a** mt-catabolic respiration, excluding mt-residual oxygen consumption, *Rox*.
- b** Total cellular O₂ consumption, including mt-*Rox*, **c** non-mt catabolic *Rox*, particularly by peroxisomal oxidases, and **e** non-mt *Rox* unrelated to catabolism.
- c** External respiration, including aerobic microbial respiration, and extracellular O₂ consumption.



MIPart by Odra Noel

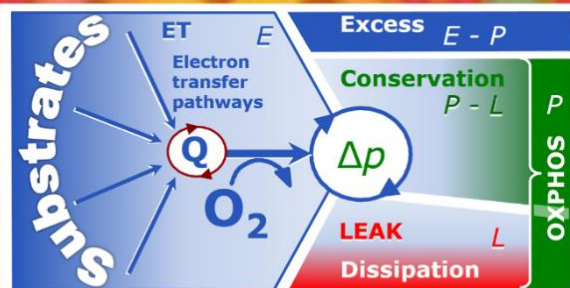
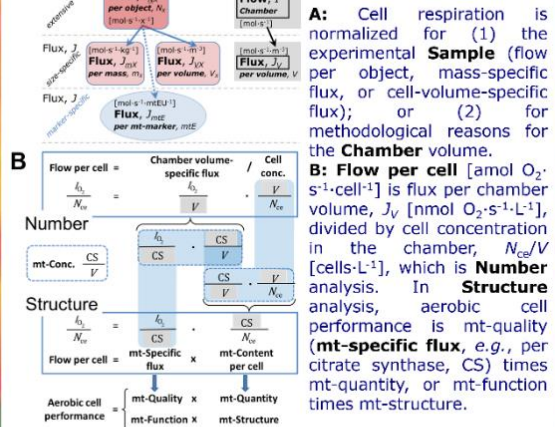


Figure 2. Respiratory states (ET, OXPHOS, LEAK) and corresponding rates (E, P, L)

Table 1. Coupling states and residual oxygen consumption in mitochondrial preparations in relation to respiration- and phosphorylation-flux, J_{kO_2} and J_{p_0} , and protonmotive force, Δp . Coupling states are established at kinetically-saturating concentrations of fuel substrates and O₂.

State	J_{kO_2}	J_{p_0}	Δp	Inducing factors	Limiting factors
LEAK	L ; low, cation leak-dependent respiration	0	max.	proton leak, slip, and cation cycling	$J_{p_0} = 0$: (1) without ADP, L_{SC} ; (2) max. ATP/ADP ratio, L_r ; or (3) inhibition of the phosphorylation-pathway, L_{Oxy}
OXPHOS	P ; high, ADP-stimulated respiration	max.	high	kinetically-saturating [ADP] and [P _i]	J_{p_0} by phosphorylation-pathway; or J_{kO_2} by ET-capacity
ET	E ; max., noncoupled respiration	0	low	optimal external uncoupler concentration for max. $J_{O_{2,E}}$	J_{kO_2} by ET-capacity
ROX	Rox ; min., residual O ₂ consumption	0	0	$J_{O_{2,Rox}}$ in non-ET-pathway oxidation reactions	inhibition of all ET-pathways; or absence of fuel substrates

Figure 3. Normalization of rate



cost EUROPEAN COOPERATION IN SCIENCE & TECHNOLOGY
Funded by the Horizon 2020 Framework Programme of the European Union

MitoEAGLE
Join
COST Action CA15203
www.mitoeagle.org/index.php/MitoEAGLE